

An arbitrarily high order unfitted finite element method for elliptic interface problems with automatic mesh generation, Part II. Piecewise-smooth interfaces*

Zhiming Chen[†] Yong Liu[‡]

Abstract.

We consider the reliable implementation of an adaptive high-order unfitted finite element method on Cartesian meshes for solving elliptic interface problems with geometrically curved singularities. We extend our previous work on the reliable cell merging algorithm for smooth interfaces to automatically generate the induced mesh for piecewise smooth interfaces. An hp a posteriori error estimate is derived for a new unfitted finite element method whose finite element functions are conforming in each subdomain. Numerical examples illustrate the competitive performance of the method.

Key words. Unfitted finite element method, Cell merging, Piecewise-smooth interface

AMS classification. 65N50, 65N30

1 Introduction

We propose an adaptive high-order unfitted finite element method on Cartesian meshes with hanging nodes for solving elliptic interface problems, which releases the work of body-fitted mesh generation and allows us to design adaptive finite element methods for solving curved geometric singularities. When the geometry of the interface and domain is simple, such as polygons or polyhedrons, it is well-known that the adaptive finite element method based on a posteriori error estimates initiated in the seminar work [6] can achieve quasi-optimal computational complexity [11, 18, 40]. The widely used newest vertex bisection algorithm [9] for simplicial meshes can guarantee the shape regularity of adaptively refined meshes starting from an initial shape regular mesh. For curved geometric singularities, however, the newest vertex bisection algorithm can no longer guarantee the shape regularity of the refined meshes. The purpose of this paper is to study an adaptive high-order finite element method

*This work is supported in part by Strategic Priority Research Program of the Chinese Academy of Sciences under the Grant No. XDB0640000, China National Key Technologies R&D Program under the grant 2019YFA0709602, China Natural Science Foundation under the grant 11831016, 12288201, 12201621 and the Youth Innovation Promotion Association (CAS).

[†]LSEC, Institute of Computational Mathematics, Academy of Mathematics and System Sciences and School of Mathematical Science, University of Chinese Academy of Sciences, Chinese Academy of Sciences, Beijing 100190, China. E-mail: zmchen@lsec.cc.ac.cn

[‡]LSEC, Institute of Computational Mathematics, Academy of Mathematics and Systems Science, Chinese Academy of Sciences, Beijing 100190, P.R. China. E-mail: yongliu@lsec.cc.ac.cn

and its reliable implementation for arbitrarily shaped piecewise C^2 -smooth interfaces in the framework of unfitted finite element methods.

The unfitted finite element method in the discontinuous Galerkin (DG) framework is first proposed in [28], which is defined on a fixed background mesh and uses different finite element functions in different cut cells that are the intersection of the elements of the mesh with the physical domains. The method has attracted considerable interest in the literature and has been extended in several directions, e.g., the cut finite element method [15, 16, 28], the hybrid high order method [14, 13], and the aggregated unfitted finite element method [7, 8]. The *small cut cell problem*, which is due to the arbitrarily small or anisotropic intersection of the interface with the elements, is solved by the ghost penalty [15, 16, 27] or by merging small cut cells with surrounding elements [32, 30, 8, 20]. We also refer to the extended finite element methods [10], the immersed boundary/interface method [39, 35, 34, 22], and the ghost fluid method [36] for other approaches in designing finite element/finite difference methods on fixed meshes.

In [19], an adaptive high-order unfitted finite element method based on hp a posteriori error estimates is proposed for the elliptic interface problem based on novel hp domain inverse estimates and the concept of the interface deviation to quantify the mesh resolution of the geometry. The method is defined on the induced mesh of an initial uniform Cartesian mesh so that each element in the induced mesh is a large element by using the idea of cell merging. A reliable algorithm to automatically generate the induced mesh is constructed in [20] for any C^2 -smooth interfaces, which is based on the concept of admissible chain of interface elements, the classification of five patterns for merging elements, and appropriately ordering in generating macro-elements from the patterns. This algorithm constitutes an important building block of this paper. We refer to [38, 37, 25] for the hp a posteriori error analysis on conforming finite element meshes and the recent work on a posteriori error analysis for immersed finite element methods [29] and the cut finite element method [17].

The main purpose of this paper is to develop a reliable algorithm to automatically generate the induced mesh for any piecewise smooth interfaces. We include a new type of proper intersection of an element with the interface, which is inevitable since the interface is locally like a curved sector around each singular point where the interface is not C^2 smooth. We design the singular pattern that merges the element including a singular point with surrounding elements such that the singular pattern is a large element and also its outlet elements have a special structure that allows us to use the reliable algorithm in [20] to merge the elements in the chain of interface elements connecting two singular patterns. The reliability of the algorithm to generate the induced mesh is also established.

The layout of the paper is as follows. In section 2 we extend the concept of the proper intersection and the large element for elements including singular points and derive an hp a posteriori error estimate for a new unfitted finite element method whose finite element functions are conforming in each subdomain. In section 3 we develop the merging algorithm for piecewise C^2 -smooth interfaces. In section 4 we report several numerical examples to illustrate the competitive performance of our adaptive method. We also include a numerical example to study the influence of the geometric modeling error by using the adaptive method developed in this paper, which confirms the theoretical result in the appendix of the paper in section 5.

2 The unfitted finite element method

Let $\Omega \subset \mathbb{R}^2$ be a Lipschitz domain with a piecewise C^2 -smooth boundary Σ . The domain Ω is divided by a piecewise C^2 -smooth interface Γ into two subdomains Ω_1, Ω_2 . We assume $\Omega_1 \subset\subset \Omega$ is a Lipschitz domain that is completely included in Ω . The intersection points of two pieces of C^2 curves of Γ or Σ are called the singular points of the interface or boundary.

We consider the following elliptic interface problem

$$-\operatorname{div}(a\nabla u) = f \quad \text{in } \Omega_1 \cup \Omega_2, \quad (2.1)$$

$$[[u]]_\Gamma = 0, \quad [[a\nabla u \cdot \mathbf{n}]]_\Gamma = 0 \quad \text{on } \Gamma, \quad u = g \quad \text{on } \Sigma, \quad (2.2)$$

where $f \in L^2(\Omega)$, $g \in H^{1/2}(\Sigma)$, \mathbf{n} is the unit outer normal to Ω_1 , and $[[v]] := v|_{\Omega_1} - v|_{\Omega_2}$ stands for the jump of a function v across the interface Γ . We assume that the coefficient $a(x)$ is positive and piecewise constant, namely, $a = a_1\chi_{\Omega_1} + a_2\chi_{\Omega_2}$, $a_1, a_2 > 0$, where χ_{Ω_i} is the characteristic function of Ω_i , $i = 1, 2$.

We assume the domain Ω is covered by a Cartesian mesh \mathcal{T} with possible hanging nodes, which is obtained by local quad refinements of an initial Cartesian mesh \mathcal{T}_0 , see Fig.2.1. A Cartesian mesh means the elements of the mesh are rectangles whose sides are parallel to the coordinate axes. We assume each element in \mathcal{T} does not intersect both Γ and Σ . The elements intersecting with the interface or boundary are called the interface elements or boundary elements. We also assume that each element can contain at most one singular point of Γ or Σ . An element that contains a singular point is called a singular element. We define the proper intersection of the interface or boundary with an element $K \in \mathcal{T}$ as follows.

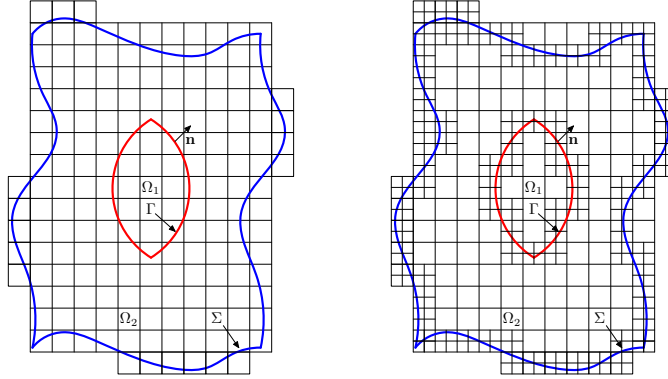


Figure 2.1: Illustration of the domain Ω and the Cartesian mesh \mathcal{T}_0 (left) and \mathcal{T} (right).

Definiton 2.1. (*Proper intersection*) *The intersection of the interface Γ or the boundary Σ with an element K is called the proper intersection if Γ or Σ intersects the boundary of K at most twice at different sides, see Fig.2.2(a-b). If K is a singular element, Γ or Σ can also intersect one side of K twice, see Fig.2.2(c).*

If Γ or Σ intersects an element at some vertex A , we regard Γ as intersecting one of the two edges originated from A at some point very close to A . If Γ or Σ is tangent to an

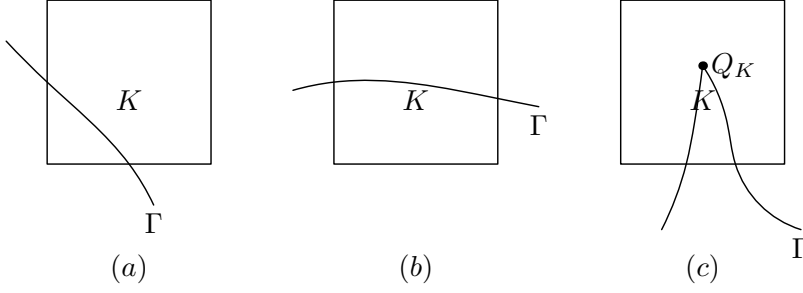


Figure 2.2: Different types of interface elements. From left to right, a type $\mathcal{T}_1, \mathcal{T}_2, \mathcal{T}_3$ element.

edge of an element, we regard Γ or Σ as being very close to the edge but not intersecting with the edge.

We call an interface or boundary element K a type $\mathcal{T}_i, i = 1, 2, 3$, element if the interface or boundary intersects the boundary of K at the two neighboring, opposite sides, or the same side, see Fig.2.2. We remark that the inclusion of the type \mathcal{T}_3 elements is important when the interface or boundary is piecewise smooth since the interface or boundary is close to a curved sector near the singular points. It is easy to see that when the mesh \mathcal{T} is locally refined near the interface and boundary, we can always assume that the intersection of Γ or Σ with each element of \mathcal{T} is the proper intersection.

From \mathcal{T} we want to construct an induced mesh \mathcal{M} , which avoids possible small intersection of the interface or boundary with the elements of the mesh. We first extend the definition of the large element in Chen et al. [19, Definition 2.1] to include type \mathcal{T}_3 interface or boundary elements. We denote $\mathcal{T}^\Gamma := \{K \in \mathcal{T} : K \cap \Gamma \neq \emptyset\}$, $\mathcal{T}^\Sigma = \{K \in \mathcal{T} : K \cap \Sigma \neq \emptyset\}$.

Definiton 2.2. (Large element) An element $K \in \mathcal{T}$ is called a large element if $K \subset \Omega_i, i = 1, 2$, or $K \in \mathcal{T}^\Gamma \cup \mathcal{T}^\Sigma$ for which the intersection of Γ or Σ with K is a proper intersection and there exists a fixed constant $\delta_0 \in (0, \frac{1}{2})$ such that $\delta_K, \tilde{\delta}_K \geq \delta_0$, where $\delta_K = \delta_K(\mathcal{T})$ is the element geometric index and $\tilde{\delta}_K = \tilde{\delta}_K(\mathcal{T})$ is the element singular index when K includes a singular point Q_K , which are defined by

$$\delta_K = \min_{\substack{i=1,2 \\ e \in \mathcal{E}_K^{\text{side}}, e \cap \Omega_i \neq \emptyset}} \frac{|e \cap \Omega_i|}{|e|}, \quad \tilde{\delta}_K = \min_{e \in \mathcal{E}_K^{\text{side}}} \frac{\text{dist}(Q_K, e)}{(|e^\perp|/2)}.$$

Here $\mathcal{E}_K^{\text{side}}$ is the set of sides of K , $\text{dist}(Q_K, e)$ is the distance of Q_K to $e \in \mathcal{E}_K^{\text{side}}$, and e^\perp is either one of two sides of K perpendicular to $e \in \mathcal{E}_K^{\text{side}}$.

The large elements including a singular point of Γ or Σ will be called *singular* large elements. The other kinds of large elements will be called *regular* large elements. If the element $K \in \mathcal{T}^\Gamma \cup \mathcal{T}^\Sigma$ is not a large element, we make the following assumption as in [20], which is inspired by Johansson and Larson [32].

Assumption (H1): For each $K \in \mathcal{T}^\Gamma \cup \mathcal{T}^\Sigma$, there exists a rectangular macro-element $M(K)$ that is a union of K and its surrounding element (or elements) such that $M(K)$ is a large element. We assume $h_{M(K)} \leq C_0 h_K$ for some fixed constant $C_0 > 0$.

This assumption can always be satisfied by using the idea of cell merging. In Chen and Liu [20], a reliable algorithm to satisfy this assumption is constructed when the interface

is C^2 smooth. For the piecewise smooth interfaces or boundaries, we will construct the merging algorithm in section 3.

In the following, we will always set $M(K) = K$ if $K \in \mathcal{T}^\Gamma \cup \mathcal{T}^\Sigma$ is a large element. Then, the induced mesh of \mathcal{T} is defined as

$$\mathcal{M} = \{M(K) : K \in \mathcal{T}^\Gamma \cup \mathcal{T}^\Sigma\} \cup \{K \in \mathcal{T} : K \not\subset M(K') \text{ for some } K' \in \mathcal{T}^\Gamma \cup \mathcal{T}^\Sigma\}.$$

We will write $\mathcal{M} = \text{Induced}(\mathcal{T})$. Note that \mathcal{M} is also a Cartesian mesh in the sense that either $M(K) \cap M(K') = \emptyset$ or $M(K) = M(K')$ for any two different elements $K, K' \in \mathcal{T}$. All elements in \mathcal{M} are large elements.

For any $K \in \mathcal{M}$, let h_K stand for the diameter of K . For $K \in \mathcal{M}^\Gamma := \{K \in \mathcal{M} : K \cap \Gamma \neq \emptyset\}$, denote $K_i = K \cap \Omega_i$, $i = 1, 2$, $\Gamma_K = \Gamma \cap K$, and let Γ intersect the sides of K at A_K, B_K . If Γ_K is smooth, we set $\Gamma_K^h = A_K B_K$, the open line segment connecting A_K, B_K . If K includes a singular point Q_K , then Γ_K is the union of two C^2 -smooth curves $\Gamma_{1K} \cup \Gamma_{2K}$ where the end points of Γ_{1K} and Γ_{2K} are A_K, Q_K and B_K, Q_K , respectively. We denote $\Gamma_{1K}^h = A_K Q_K$, $\Gamma_{2K}^h = Q_K B_K$, and $\Gamma_K^h = \Gamma_{1K}^h \cup Q_K \cup \Gamma_{2K}^h$. In either case, Γ_K^h divides K into two polygons K_1^h, K_2^h . As the consequence of that K is a large element, we have the following lemma, which can be easily proved and we omit the details.

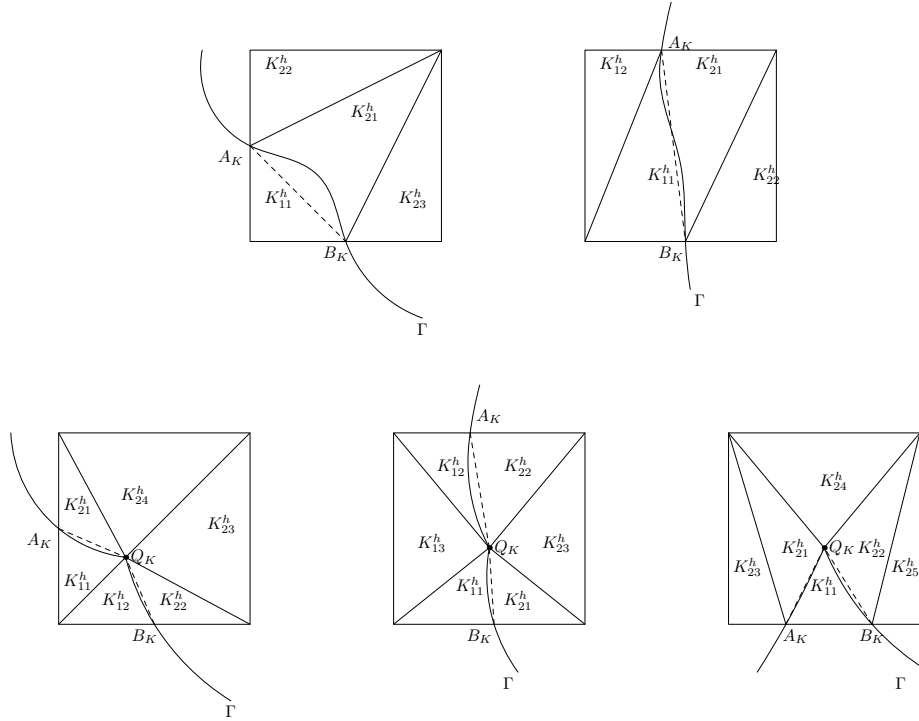


Figure 2.3: Illustration of K_{ij}^h of the *regular* interface large elements (top) or *singular* interface large elements. Γ_{iK}^h are denoted by the dashed line, $i = 1, 2, j = 1, \dots, J_i^K$.

Lemma 2.1. *Let $K \in \mathcal{M}^\Gamma$. Then for $i = 1, 2$, K_i^h is the union of triangles K_{ij}^h , $j = 1, \dots, J_i^K$, $1 \leq J_i^K \leq 5$, such that if K is a regular large element, K_{ij}^h has one vertex at A_K^i that is included in Ω_i and has the maximum distance to Γ_K^h , and if K is a singular*

large element, K_{ij}^h has one vertex at Q_K . The other two vertices of K_{ij}^h , $j = 1, \dots, J_i^K$, $i = 1, 2$, are A_K, B_K or the vertices of K in Ω_i , see Fig.2.3. Moreover, K_{ij}^h , $j = 1, \dots, J_i^K$, $i = 1, 2$, are shape regular in the sense that the radius of the maximal inscribed circle of K_{ij}^h is bounded below by $c_0 h_K$ for some constant $c_0 > 0$ depending only on δ_0 in Definition 2.2.

If K_{ij}^h has one side as Γ_K^h or Γ_{jK}^h , $j = 1, 2$, we define \tilde{K}_{ij}^h as the curved triangle bounded by the other two sides of K_{ij}^h and one curved side Γ_K or Γ_{jK}^h , $j = 1, 2$. If K_{ij}^h does not have a side as Γ_K^h or Γ_{jK}^h , $j = 1, 2$, we define $\tilde{K}_{ij}^h = K_{ij}^h \cap \bar{K}_i$. Then we have

$$K = K_1 \cup \Gamma_K \cup K_2, \quad K_i = \text{the interior of } \overline{\cup_{j=1}^{J_i^K} \tilde{K}_{ij}^h}, \quad i = 1, 2.$$

For $K \in \mathcal{M}^\Gamma$, we set $\mathcal{M}(K) = \{K_{ij}^h : i = 1, 2, j = 1, \dots, J_i^K\}$, $\tilde{\mathcal{M}}(K) = \{\tilde{K}_{ij}^h : i = 1, 2, j = 1, \dots, J_i^K\}$, and $\sigma_K : \mathcal{M}(K) \rightarrow \tilde{\mathcal{M}}(K)$ the mapping $\sigma_K(K_{ij}^h) = \tilde{K}_{ij}^h$, $j = 1, \dots, J_i^K$, $i = 1, 2$.

Similarly, for $K \in \mathcal{M}^\Sigma := \{K \in \mathcal{M} : K \cap \Sigma \neq \emptyset\}$, we denote $\Sigma_K = \Sigma \cap K$ and let Σ intersect K at two points A_K, B_K . If Σ is smooth in K , set $\Sigma_K^h = A_K B_K$, and if K is a singular boundary element, denote $\Sigma_{1K}^h = A_K Q_K$, $\Sigma_{2K}^h = B_K Q_K$, and $\Sigma_K^h = \Sigma_{1K}^h \cup Q_K \cup \Sigma_{2K}^h$. We let Σ_{1K} the curve of Σ with the end points A_K, Q_K and Σ_{2K} the curve of Σ with the end points B_K, Q_K so that $\Sigma_K = \Sigma_{1K} \cup Q_K \cup \Sigma_{2K}$. K^h is the polygon bounded by Σ_K^h and $\partial K \cap \Omega$. The proof of the following lemma is also omitted.

Lemma 2.2. *Let $K \in \mathcal{M}^\Sigma$. Then K^h is the union of triangles K_j^h , $j = 1, \dots, J^K$, $1 \leq J^K \leq 5$, such that if K is a regular large element, K_j^h has one vertex at A_K in Ω that has the maximum distance to Σ_K^h , and if K is a singular large element, K_j^h has one vertex at Q_K . The other two vertices of K_j^h , $j = 1, \dots, J^K$, are A_K, B_K or the vertices of K in Ω . Moreover, K_j^h , $j = 1, \dots, J^K$, are shape regular in the sense that the radius of the maximal inscribed circle of K_j^h is bounded below by $c_0 h_K$ for some constant $c_0 > 0$ depending only on δ_0 in Definition 2.2.*

Again if K_j^h has one side as Σ_K^h or Σ_{jK}^h , $j = 1, 2$, we define \tilde{K}_j^h as the curved triangle bounded by the other two sides of K_j^h and one curved side Σ_K or Σ_{jK}^h , $j = 1, 2$. If K_j^h does not have a side as Σ_K^h or Σ_{jK}^h , $j = 1, 2$, we define $\tilde{K}_j^h = K_j^h \cap \bar{\Omega}$. Then we have

$$K \cap \Omega = \text{the interior of } \overline{\cup_{j=1}^{J^K} \tilde{K}_j^h}.$$

For $K \in \mathcal{T}^\Sigma$, we denote $\mathcal{M}(K) = \{K_j^h : j = 1, \dots, J^K\}$, $\tilde{\mathcal{M}}(K) = \{\tilde{K}_j^h : j = 1, \dots, J^K\}$, and $\sigma_K : \mathcal{M}(K) \rightarrow \tilde{\mathcal{M}}(K)$ the mapping $\sigma_K(K_j^h) = \tilde{K}_j^h$, $j = 1, \dots, J^K$.

For $i = 1, 2$, let \mathcal{M}_i be the set of elements $K \in \mathcal{M}$ included in Ω_i , the triangles $T \in \mathcal{T}(K)$, $T \subset K_i^h$ for all elements $K \in \mathcal{M}^\Gamma$, and the triangles $T \subset K^h$ for all elements $K \in \mathcal{M}^\Sigma$. Then \mathcal{M}_i is a shape regular body-fitted mixed rectangular and triangular mesh of Ω_i , and $\mathcal{M}_1 \cup \mathcal{M}_2$ is a shape regular body-fitted mixed rectangular and triangular mesh of Ω .

The concept of interface deviation introduced in [19] plays an important role in our subsequent analysis. Roughly speaking, the interface deviation measures how far Γ_K deviates from Γ_K^h or Γ_{jK} from Γ_{jK}^h , $j = 1, 2$. We now extend this concept to include also the type \mathcal{T}_3 interface and boundary elements.

Definiton 2.3. For any $K \in \mathcal{M}^\Gamma \cup \mathcal{M}^\Sigma$, the interface or boundary deviation η_K is defined as

$$\eta_K = \max_{\tilde{T} \in \widetilde{\mathcal{M}}(K)^*} \frac{\text{dist}_H(E_T^h, E_T)}{\text{dist}(A_T, E_T^h)},$$

where $\widetilde{\mathcal{M}}(K)^*$ is the set of elements $\tilde{T} \in \widetilde{\mathcal{M}}(K)$ having one curved side E_T , E_T^h is the straight segment connecting the end points of E_T , and A_T is the vertex of T opposite to E_T . Here $\text{dist}_H(\Gamma_1, \Gamma_2) = \max_{x \in \Gamma_1} (\min_{y \in \Gamma_2} |x - y|)$ and $\text{dist}(A, \Gamma_1)$ is the distance of a point A to the set Γ_1 .

It is known [19] that $\eta_K \leq Ch_K$. The following assumption, which can be viewed as a variant of the conditions of the mesh resolving the geometry of the interface or boundary, can be easily satisfied if the mesh is locally refined near the interface or boundary.

Assumption (H2): For any $K \in \mathcal{M}^\Gamma \cup \mathcal{M}^\Sigma$, $\eta_K \leq \eta_0$ for some $\eta_0 \in (0, 1/2)$.

The study in [20] suggests that one should choose $\eta_0 \leq 0.1/[p(p+1)]$ in practice to control the condition number of the stiffness matrix of the unfitted finite element method.

Since the mesh \mathcal{T} may have hanging nodes, we introduce an important concept of K -mesh introduced in Babuška and Miller [5] for the Cartesian mesh \mathcal{T} . Let \mathcal{N}^0 be the set of conforming nodes of \mathcal{T} , which are the vertices of the elements either located on the boundary Σ or shared by the four elements to which they belong. For each conforming node P , we denote by $\psi_P \in H^1(\Omega^h)$, where $\Omega^h = (\cup_{K \in \mathcal{T}} \bar{K})^\circ$, the element-wise bilinear function that satisfies $\psi_P(Q) = \delta_{PQ} \forall Q \in \mathcal{N}^0$. Here δ_{PQ} is the Kronecker delta. We impose the following K -mesh condition on the mesh \mathcal{T} and refer to Bonito and Nochetto [12, §6] for a refinement algorithm to enforce the assumption.

Assumption (H3): There exists a constant $C > 0$ independent of h_K for all $K \in \mathcal{T}$ such that for any conforming node $P \in \mathcal{N}^0$, $\text{diam}(\text{supp}(\psi_P)) \leq C \min_{K \in \mathcal{T}_P} h_K$, where $\mathcal{T}_P = \{K \in \mathcal{T} : K \subset \text{supp}(\psi_P)\}$.

For any $p \geq 1$ and any Lipschitz domain $D \subset \mathbb{R}^d$, $d \geq 1$, we denote by $P_p(D)$ the space of polynomials of degree at most p in D and $Q_p(D)$ the space of polynomials of degree at most p for each variable in D . The unfitted finite element space in Hansbo and Hansbo [28] and also used in [19], [20] is

$$\mathbb{H}_p(\mathcal{M}) = \{v \in L^2(\Omega) : v = v_1 \chi_{\Omega_1} + v_2 \chi_{\Omega_2}, v_1|_K, v_2|_K \in Q_p(K), K \in \mathcal{M}\}.$$

The finite element functions in this space in general cannot be conforming in each subdomain Ω_1, Ω_2 . In Chen et al. [21, Lemma 2.3], it is shown that the mesh \mathcal{M} constructed by [20, Algorithm 6] always satisfies the following compatibility assumption in each subdomain. This allows us to propose a new unfitted finite element space that is conforming in each domain Ω_1, Ω_2 .

Assumption (H4): If $e = \partial G \cap \partial G'$, $G, G' \in \mathcal{M}_i$, and F, F' be respectively the side of G, G' including e , then either $F \subset F'$ or $F' \subset F$.

We introduce the following finite element spaces on the interface or boundary elements

$$X_p(K) = \{v \in H^1(K_1 \cup K_2) : v|_{\tilde{T}} \in P_p(\tilde{T}), \tilde{T} \in \widetilde{\mathcal{M}}(K)\} \quad \forall K \in \mathcal{M}^\Gamma,$$

$$X_p(K) = \{v \in H^1(K \cap \Omega) : v|_{\tilde{T}} \in P_p(\tilde{T}), \tilde{T} \in \widetilde{\mathcal{M}}(K)\} \quad \forall K \in \mathcal{M}^\Sigma.$$

We also introduce the finite element spaces

$$\begin{aligned} U_p(K) &= \{v \in H^1(K_1^h \cup K_2^h) : v|_T \in P_p(T), T \in \mathcal{M}(K)\} \quad \forall K \in \mathcal{M}^\Gamma, \\ U_p(K) &= \{v \in H^1(K^h) : v|_T \in P_p(T), T \in \mathcal{M}(K)\} \quad \forall K \in \mathcal{M}^\Sigma. \end{aligned}$$

The degrees of freedom of the finite elements functions in $X_p(K)$, $K \in \mathcal{M}^\Gamma \cup \mathcal{M}^\Sigma$, can be defined by using the degrees of freedom of the finite elements functions in $U_p(K)$ via the following natural extension $\mathbb{E}_K : U_p(K) \rightarrow X_p(K)$ such that for any $\phi \in U_p(K)$,

$$\mathbb{E}_K(\phi)|_{T \cap \tilde{T}} = \phi|_{T \cap \tilde{T}} \quad \forall T \in \mathcal{M}(K), \quad \tilde{T} = \sigma_K(T) \in \widetilde{\mathcal{M}}(K). \quad (2.3)$$

Thanks to the compatibility assumption of the mesh \mathcal{M}_i in the subdomain Ω_i , $i = 1, 2$, we can define the following unfitted finite element space, which is conforming in each subdomain Ω_1, Ω_2 ,

$$\begin{aligned} \mathbb{X}_p(\mathcal{M}) &:= \{v \in H^1(\Omega_1 \cup \Omega_2) : v|_K \in X_p(K) \quad \forall K \in \mathcal{M}^\Gamma \cup \mathcal{M}^\Sigma, \\ &\quad v|_K \in Q_p(K) \quad \forall K \in \mathcal{M}, K \subset \Omega_i, i = 1, 2\}. \end{aligned}$$

In [19, Lemma 2.4], an hp domain inverse estimate is proved for unfitted finite element functions in $\mathbb{H}_p(\mathcal{M})$. The following domain inverse estimates for $\mathbb{X}_p(\mathcal{M})$ finite element functions are shown in [21, Lemma 2.5] by modifying the argument in [19, Lemma 2.4].

Lemma 2.3. *Let $K \in \mathcal{M}^\Gamma \cup \mathcal{M}^\Sigma$. Then there exists a constant C independent of p , h_K and η_K for all $K \in \mathcal{M}$ such that for $i = 1, 2$,*

$$\|\nabla v\|_{L^2(K_i)} \leq Cp^2 h_K^{-1} \Theta_K^{1/2} \|v\|_{L^2(K_i)}, \quad \|v\|_{L^2(\partial K_i)} \leq Cph_K^{-1/2} \Theta_K^{1/2} \|v\|_{L^2(K_i)} \quad \forall v \in X_p(K),$$

where

$$\Theta_K = T \left(\frac{1 + 3\eta_K}{1 - \eta_K} \right)^{2p+3} \quad \forall K \in \mathcal{M}^\Gamma \cup \mathcal{M}^\Sigma.$$

Here $\Upsilon(t) = t + \sqrt{t^2 - 1} \quad \forall t \geq 1$.

Now we turn to the introduction of the unfitted finite element method. Let $\mathcal{E} = \mathcal{E}^{\text{side}} \cup \mathcal{E}^{\text{bdy}}$, where $\mathcal{E}^{\text{side}} := \{e = \partial K \cap \partial K' : K, K' \in \mathcal{M}\} \cup \{e = \partial \tilde{T} \cap \partial \tilde{T}' : \tilde{T}, \tilde{T}' \in \widetilde{\mathcal{M}}(K), K \in \mathcal{M}^\Gamma \cup \mathcal{M}^\Sigma\}$ and $\mathcal{E}^{\text{bdy}} := \{\Sigma_K = \Sigma \cap K : K \in \mathcal{M}\}$. Set $\mathcal{E}^\Gamma := \{\Gamma_K = \Gamma \cap K : K \in \mathcal{M}\}$. Notice that $\mathcal{E}^\Gamma \subset \mathcal{E}^{\text{side}}$ but $\mathcal{E}^{\text{bdy}} \not\subset \mathcal{E}^{\text{side}}$. For any subset $\widehat{\mathcal{M}} \subset \mathcal{M}$ and $\widehat{\mathcal{E}} \subset \mathcal{E}$, we use the notation

$$(u, v)_{\widehat{\mathcal{M}}} = \sum_{K \in \widehat{\mathcal{M}}} (u, v)_K, \quad \langle u, v \rangle_{\widehat{\mathcal{E}}} = \sum_{e \in \widehat{\mathcal{E}}} \langle u, v \rangle_e,$$

where $(\cdot, \cdot)_K$ and $\langle \cdot, \cdot \rangle_e$ denote the inner product of $L^2(K)$ and $L^2(e)$, respectively.

For any $e \in \mathcal{E}$, we fix a unit normal vector \mathbf{n}_e of e with the convention that \mathbf{n}_e is the unit outer normal to $\partial\Omega$ if $e \in \mathcal{E}^{\text{bdy}}$, and \mathbf{n}_e is the unit outer normal to $\partial\Omega_1$ if $e \in \mathcal{E}^\Gamma$.

Define the normal function $\mathbf{n}|_e = \mathbf{n}_e \forall e \in \mathcal{E}$. For any $v \in H^1(\mathcal{M}) := \{v \in L^2(\Omega) : v|_K \in H^1(K), K \in \mathcal{M}\}$, we define the jump operator of v across e :

$$[[v]]_e := v^- - v^+ \quad \forall e \in \mathcal{E}^{\text{side}}, \quad \llbracket v \rrbracket_e := v^- \quad \forall e \in \mathcal{E}^{\text{bdy}}, \quad (2.4)$$

where $v^\pm(\mathbf{x}) := \lim_{\varepsilon \rightarrow 0^+} v(\mathbf{x} \pm \varepsilon \mathbf{n}_e)$ for any $\mathbf{x} \in e$. The mesh function $h|_e = (h_K + h_{K'})/2$ if $e = \partial K \cap \partial K', K, K' \in \mathcal{M}$, and $h|_e = h_K$ if $e = \partial \tilde{T} \cap \partial \tilde{T}', \tilde{T}, \tilde{T}' \in \tilde{\mathcal{M}}(K), K \in \mathcal{M}^\Gamma \cup \mathcal{M}^\Sigma$ or $e = K \cap \Sigma \in \mathcal{E}^{\text{bdy}}$.

For any $v \in H^1(\mathcal{M}), g \in L^2(\Sigma)$, we define the liftings $\mathbf{L}(v) \in [\mathbb{X}_p(\mathcal{M})]^2, \mathbf{L}_1(g) \in [\mathbb{X}_p(\mathcal{M})]^2$ such that

$$(w, \mathbf{L}(v))_{\mathcal{M}} = \langle w^- \cdot \mathbf{n}, [[v]] \rangle_{\mathcal{E}^\Gamma \cup \mathcal{E}^{\text{bdy}}}, \quad (w, \mathbf{L}_1(g))_{\mathcal{M}} = \langle w \cdot \mathbf{n}, g \rangle_{\mathcal{E}^{\text{bdy}}} \quad \forall w \in [\mathbb{X}_p(\mathcal{M})]^2. \quad (2.5)$$

Our unfitted finite element method is to find $U \in \mathbb{X}_p(\mathcal{M})$ such that

$$a_h(U, v) = F_h(v) \quad \forall v \in \mathbb{X}_p(\mathcal{M}), \quad (2.6)$$

where the bilinear form $a_h : H^1(\mathcal{M}) \times H^1(\mathcal{M}) \rightarrow \mathbb{R}$, and the functional $F_h : H^1(\mathcal{M}) \rightarrow \mathbb{R}$ are given by

$$\begin{aligned} a_h(v, w) = & (a(\nabla_h v - \mathbf{L}(v)), \nabla_h w - \mathbf{L}(w))_{\mathcal{M}} + \langle \alpha [[v]], [[w]] \rangle_{\mathcal{E}^\Gamma \cup \mathcal{E}^{\text{bdy}}} \\ & + \langle p^{-2} h \nabla_T [[v]], \nabla_T [[w]] \rangle_{\mathcal{E}^\Gamma \cup \mathcal{E}^{\text{bdy}}}, \end{aligned} \quad (2.7)$$

$$\begin{aligned} F_h(v) = & (f, v)_{\mathcal{M}} - (a \mathbf{L}_1(g), \nabla_h v - \mathbf{L}(v))_{\mathcal{M}} + \langle \alpha g, v \rangle_{\mathcal{E}^{\text{bdy}}} \\ & + \langle p^{-2} h \nabla_T g, \nabla_T v \rangle_{\mathcal{E}^{\text{bdy}}}, \end{aligned} \quad (2.8)$$

where ∇_T is the surface gradient on Γ or Σ . The interface penalty function $\alpha \in L^\infty(\mathcal{E}^\Gamma \cup \mathcal{E}^{\text{bdy}})$ is

$$\alpha|_e = \alpha_0 \hat{a}_e \hat{\Theta}_e h_e^{-1} p^2 \quad \forall e \in \mathcal{E}^\Gamma \cup \mathcal{E}^{\text{bdy}}, \quad (2.9)$$

where $\alpha_0 > 0$ is a fixed constant, $\hat{a}_e = \max\{a_K : e \cap \bar{K} \neq \emptyset\}$, $\hat{\Theta}_e = \max\{\Theta_K : e \cap \bar{K} \neq \emptyset\}$. Here $a_K = \|a\|_{L^\infty(K)}$. We remark that (2.6) is a variant of local discontinuous Galerkin method in Cockburn and Shu [24] on the mesh with curved elements. The stabilization term $\langle \alpha [[v]], [[w]] \rangle_{\mathcal{E}^\Gamma}$ in (2.6) plays the key role in weakly capturing the jump behavior of the finite element solution at the interface. The boundary condition is also weakly appeared in the (2.6) through the penalty form.

By Lemma 2.3, we deduce easily that

$$\|a^{1/2} \mathbf{L}(v)\|_{\mathcal{M}} \leq C \|\alpha^{1/2} [[v]]\|_{\mathcal{E}^\Gamma \cup \mathcal{E}^{\text{bdy}}}, \quad (2.10)$$

where the constant C is independent of p, h_K and η_K for all $K \in \mathcal{M}$, and the coefficient a . The stability of the bilinear form $a_h(\cdot, \cdot)$ can be proved by using (2.10) and the standard argument in e.g., [19, Theorem 2.1], from which, together with the hp interpolation operator in [21, Theorem 2.1], one can derive an hp a priori error estimate as e.g., in [20, Theorem 2.1]. Here we do not elaborate on the details.

Our main goal in this section is to derive the a posteriori error estimate for the solution U of the problem (2.6), which is the basis for designing adaptive finite element methods for resolving the geometric singularities of the interface and boundary. The key ingredient

in the a posteriori error analysis is an hp -quasi-interpolation for H^1 functions in $X_p(\mathcal{M})$ that we now define. Denote $\Omega_h = (U_{K \in \mathcal{M}} \bar{K})^\circ$ be the domain covering Ω and $\mathbb{V}_p(\mathcal{M}) = \Pi_{K \in \mathcal{M}} Q_p(K)$. In [19, Lemma 3.1], an hp -quasi-interpolation operator $\Pi_{hp} : H^1(\Omega_h) \rightarrow \mathbb{V}_p(\mathcal{M}) \cap H^1(\Omega_h)$ on K -meshes is constructed by extending the idea in Melenk [37] for the hp -quasi-interpolation on conforming meshes. It is shown in [19, Lemma 3.1] that for any $v \in H^1(\Omega_h)$, there exists a constant C independent of p , h_K for all $K \in \mathcal{M}$ such that

$$\|D^m(v - \Pi_{hp}v)\|_{L^2(K)} \leq C(h_K/p)^{1-m} \|\nabla v\|_{L^2(\omega(K))}, \quad m = 0, 1, \quad (2.11)$$

$$\|v - \Pi_{hp}v\|_{L^2(\partial K)} \leq C(h_K/p)^{1/2} \|\nabla v\|_{L^2(\omega(K))}, \quad (2.12)$$

where $\omega(K) = \{K' \in \mathcal{M} : K' \subset \text{supp}(\psi_P) \ \forall P \in \mathcal{N}^0 \text{ such that } \psi_P|_K \neq 0\}$. By Assumption (H3), $\text{diam}(\omega(K)) \leq Ch_K$.

Lemma 2.4. *There exists a quasi-interpolation operator $\pi_{hp} : H^1(\Omega) \rightarrow \mathbb{X}_p(\mathcal{M})$ such that for any $v \in H^1(\Omega)$ and $K \in \mathcal{M}$,*

$$\|D^m(v - \pi_{hp}v)\|_{L^2(K)} \leq C(h_K/p)^{1-m} \|\nabla v\|_{L^2(\omega(K))}, \quad m = 0, 1, \quad (2.13)$$

$$\|v - \pi_{hp}v\|_{L^2(\partial K)} \leq C(h_K/p)^{1/2} \|\nabla v\|_{L^2(\omega(K))}. \quad (2.14)$$

Moreover, for any $\tilde{T} \in \tilde{\mathcal{M}}(K)$, $K \in \mathcal{M}^\Gamma \cup \mathcal{M}^\Sigma$,

$$\|v - \pi_{hp}v\|_{L^2(\partial \tilde{T})} \leq C(h_K/p)^{1/2} \|\nabla v\|_{L^2(\omega(K))}. \quad (2.15)$$

The constant C is independent of p , h_K and η_K for all $K \in \mathcal{M}$.

Proof. We first recall the following well-known multiplicative trace inequality

$$\|v\|_{L^2(\partial T)} \leq Ch_T^{-1/2} \|v\|_{L^2(T)} + C \|v\|_{L^2(T)}^{1/2} \|\nabla v\|_{L^2(T)}^{1/2} \quad \forall v \in H^1(T), T \in \mathcal{M}(K). \quad (2.16)$$

Next, for any $K \in \mathcal{M}^\Gamma$, we have the following trace inequality on curved domains in Xiao et al. [42]

$$\|v\|_{L^2(\Gamma_K)} \leq C \|v\|_{L^2(K_i)}^{1/2} \|v\|_{H^1(K_i)}^{1/2} + \|v\|_{L^2(\partial K_i \setminus \Gamma_K)} \quad \forall v \in H^1(K), i = 1, 2. \quad (2.17)$$

A similar inequality for Σ_K , $K \in \mathcal{M}^\Sigma$ also holds. Then (2.15) follows from (2.13)-(2.14) by using (2.16)-(2.17).

Now we prove (2.13)-(2.14). Denote by $\tilde{v} \in H^1(\mathbb{R}^2)$ the Stein extension of $v \in H^1(\Omega)$ such that $\|\tilde{v}\|_{H^1(\mathbb{R}^2)} \leq C \|v\|_{H^1(\Omega)}$. For $p = 2k$ or $p = 2k + 1$, $k \geq 1$, since $Q_k(K) \subset P_{2k}(K)$, by setting $\pi_{hp}v = \Pi_{hk}(\tilde{v}|_{\Omega_h})$ we obtain (2.13)-(2.14) by (2.11)-(2.12).

It remains the case when $p = 1$. For any $v \in H^1(\Omega)$, we let $v_h = \Pi_{h1}(\tilde{v}|_{\Omega_h}) \in \mathbb{V}_1(\mathcal{M}) \cap H^1(\Omega_h)$. By (2.11) we have

$$\|D^m(v - v_h)\|_{L^2(K)} \leq Ch_K^{1-m} \|\nabla v\|_{L^2(\omega(K))}, \quad m = 0, 1. \quad (2.18)$$

Thus if K is included in Ω_i , $i = 1, 2$, we define $\pi_{h1}v = v_h$ in K , which satisfies the desired estimates (2.13)-(2.14). For any $K \in \mathcal{M}^\Gamma \cup \mathcal{M}^\Sigma$, we notice that v_h is bilinear in K that is not in $X_1(K)$. Let $v_K = \frac{1}{|K|} \int_K v dx$. Then the standard scaling argument yields

$$\|D^m(v - v_K)\|_{L^2(K)} \leq Ch_K^{1-m} \|\nabla v\|_{L^2(K)}, \quad m = 0, 1. \quad (2.19)$$

Now we are going to lift the piecewise linear polynomial $v_h - v_K$ on ∂K to a finite element function in $U_1(K)$. We only consider the case shown in the right of Fig.2.3. The other cases are similar. By the classical polynomial lifting result in Babuška et al. [4, Lemma 7.1] and the scaling argument, we know that there exists a $F_{11} \in P_1(K_{11}^h)$ such that $F_{11} = v_h - v_K$ on $A_K B_K$ and for $m = 0, 1$,

$$\begin{aligned} \|D^m F_{11}\|_{L^2(K_{11}^h)} &\leq Ch_K^{1-m} (h_K^{-1/2} \|v_h - v_K\|_{L^2(A_K B_K)} + |v_h - v_K|_{H^{1/2}(A_K B_K)}) \\ &\leq Ch_K^{1-m} \|v_h - v_K\|_{H^1(K)}. \end{aligned}$$

This implies by (2.18)-(2.19) that $\|D^m F_{11}\|_{L^2(K_{11}^h)} \leq Ch_K^{1-m} \|\nabla v\|_{L^2(\omega(K))}$, $m = 0, 1$. Similarly, by the polynomial lifting in [4, Lemma 7.2] for two sides, there exist $F_{23} \in P_1(K_{23}^h)$ and $F_{25} \in P_1(K_{25}^h)$ such that $F_{23} = v_h - v_K$ on $\partial K \cap \partial K_{23}^h$, $F_{25} = v_h - v_K$ on $\partial K \cap \partial K_{25}^h$, and $\|D^m F_{23}\|_{L^2(K_{23}^h)} + \|D^m F_{25}\|_{L^2(K_{25}^h)} \leq Ch_K^{1-m} \|\nabla v\|_{L^2(\omega(K))}$, $m = 0, 1$. Since $F_{23} = F_{11}$ at A_K , $F_{25} = F_{11}$ at B_K , we can define linear lifting functions $F_{21} \in P_1(K_{21}^h)$, $F_{22} \in P_1(K_{22}^h)$ and then $F_{24} \in P_1(K_{24}^h)$ such that $F_{24} = v_h - v_K$ on $\partial K \cap K_{24}^h$ and

$$\|D^m F_{21}\|_{L^2(K_{21}^h)} + \|D^m F_{22}\|_{L^2(K_{22}^h)} + \|D^m F_{24}\|_{L^2(K_{24}^h)} \leq Ch_K^{1-m} \|\nabla v\|_{L^2(\omega(K))}, \quad m = 0, 1.$$

Now define $F \in U_1(K)$ by $F|_{K_{ij}^h} = F_{ij}$, $i = 1, 2, j = 1, \dots, J_i^K$, then we have $\|D^m F\|_{L^2(K)} \leq Ch_K^{1-m} \|\nabla v\|_{L^2(\omega(K))}$. Let $\pi_{h1} v = v_K + \mathbb{E}_K(F)$, where $\mathbb{E}_K(F)$ is defined in (2.3). Then $\pi_{h1} v \in X_1(K)$, $\pi_{h1} v = v_h$ on ∂K , and since $p = 1$, by Lemma 2.3 and (2.19) we know that

$$\begin{aligned} \|D^m(v - \pi_{h1} v)\|_{L^2(K)} &\leq \|D^m(v - v_K)\|_{L^2(K)} + \|D^m \mathbb{E}_K(F)\|_{L^2(K)} \\ &\leq \|D^m(v - v_K)\|_{L^2(K)} + C \|D^m F\|_{L^2(K)} \\ &\leq Ch_K^{1-m} \|\nabla v\|_{L^2(\omega(K))}, \quad m = 0, 1. \end{aligned}$$

This shows (2.13). The estimate (2.14) follows from (2.13) by the multiplicative trace inequality. This completes the proof. \square

Let $U \in \mathbb{X}_p(\mathcal{M})$ be the solution of the problem (2.6), we define the element and jump residuals

$$R(U)|_K = f + \operatorname{div}_h(a \nabla_h U) \quad \forall K \in \mathcal{M}, \quad J(U)|_e = \llbracket a \nabla_h U \cdot \mathbf{n} \rrbracket_e \quad \forall e \in \mathcal{E}^{\text{side}}.$$

We also define the functions $\Lambda : \Pi_{K \in \mathcal{M}} L^2(K) \rightarrow \mathbb{R}$ and $\hat{\Lambda} : \Pi_{e \in \mathcal{E}} L^2(e) \rightarrow \mathbb{R}$ as

$$\Lambda|_K = \|a^{1/2}\|_{L^\infty(K)} \|a^{-1/2}\|_{L^\infty(\omega(K))} \quad \forall K \in \mathcal{M}, \quad \hat{\Lambda}|_e = \max\{\Lambda_K : e \cap \bar{K} \neq \emptyset\} \quad \forall e \in \mathcal{E}.$$

Lemma 2.5. *Let $w \in H_0^1(\Omega)$ and $w_h = \pi_{hp} w \in \mathbb{X}_p(\mathcal{M})$ be defined in Lemma 2.4. Define $\zeta \in L^\infty(\Omega_h)$ by $\zeta|_K = p^{1/2} \Theta_K^{1/2} \Lambda_K \quad \forall K \in \mathcal{M}$. Then there exists a constant C independent of p , h_K and η_K for all $K \in \mathcal{M}$, and the coefficient a such that $\|a^{1/2} \zeta^{-1} \mathbf{L}(w_h)\|_{\mathcal{M}} \leq C \|a^{1/2} \nabla w\|_{\mathcal{M}}$.*

Proof. By the definition of the lifting operator in (2.5) we know that $(v, \mathbf{L}(w_h))_{\mathcal{M}} = \langle v^- \cdot \mathbf{n}, \llbracket w_h \rrbracket \rangle_{\mathcal{E}^{\text{r}} \cup \mathcal{E}^{\text{bdy}}} \quad \forall v \in [\mathbb{X}_p(\mathcal{M})]^2$. By taking $v = a \zeta^{-2} \mathbf{L}(w_h) \in [\mathbb{X}_p(\mathcal{M})]^2$, we have

$$\|a^{1/2} \zeta^{-1} \mathbf{L}(w_h)\|_{\mathcal{M}}^2 = \sum_{K \in \mathcal{M}^\Gamma} \langle [a \zeta^{-2} \mathbf{L}(w_h)]^- \cdot \mathbf{n}, \llbracket w_h \rrbracket \rangle_{\Gamma_K} + \sum_{K \in \mathcal{M}^\Sigma} \langle [a \zeta^{-2} \mathbf{L}(w_h)]^- \cdot \mathbf{n}, \llbracket w_h \rrbracket \rangle_{\Sigma_K}. \quad (2.20)$$

By Lemma 2.3 and Lemma 2.4, for any $K \in \mathcal{M}^\Gamma$,

$$\begin{aligned} \langle [a\zeta^{-2}\mathbf{L}(w_h)]^- \cdot \mathbf{n}, \llbracket w_h \rrbracket \rangle_{\Gamma_K} &\leq C a_K^{1/2} (\zeta|_K)^{-2} p^{1/2} \Theta_K^{1/2} \|a^{1/2}\mathbf{L}(w_h)\|_{L^2(K)} \|\nabla w\|_{L^2(\omega(K))} \\ &\leq C \|a^{1/2}\zeta^{-1}\mathbf{L}(w_h)\|_{L^2(K)} \|a^{1/2}\nabla w\|_{L^2(\omega(K))}. \end{aligned}$$

Similarly, for any $K \in \mathcal{M}^\Sigma$,

$$\langle [a\zeta^{-2}\mathbf{L}(w_h)]^- \cdot \mathbf{n}, \llbracket w_h \rrbracket \rangle_{\Sigma_K} \leq C \|a^{1/2}\zeta^{-1}\mathbf{L}(w_h)\|_{L^2(K)} \|a^{1/2}\nabla w\|_{L^2(\omega(K))}.$$

This completes the proof by inserting above two estimates to (2.20). \square

For any $v \in H^1(\mathcal{M})$, we define the following DG norm

$$\|v\|_{\text{DG}}^2 = \|a^{1/2}\nabla v\|_{\mathcal{M}}^2 + \|\alpha^{1/2}\llbracket v \rrbracket\|_{\mathcal{E}^\Gamma \cup \mathcal{E}^{\text{bdy}}}^2 + \|p^{-1}h^{1/2}\nabla_T \llbracket v \rrbracket\|_{\mathcal{E}^\Gamma \cup \mathcal{E}^{\text{bdy}}}^2.$$

The following theorem is the main result of this section.

Theorem 2.1. *Let $u \in H^1(\Omega)$ be the weak solution of (2.1)-(2.2) with $g \in H^1(\partial\Omega)$ and $U \in \mathbb{X}_p(\mathcal{M})$ be the solution of (2.6). Then there exists a constant C independent of p , h_K and η_K for all $K \in \mathcal{M}$, and the coefficient a such that*

$$\|u - U\|_{\text{DG}} \leq C \left(\sum_{K \in \mathcal{M}} \xi_K^2 \right)^{1/2},$$

where for each $K \in \mathcal{M}$, the local a posteriori error estimator

$$\begin{aligned} \xi_K^2 &= \left(\|a^{-1/2}(h/p)\Lambda R(U)\|_K^2 + \|\hat{a}^{-1/2}(h/p)^{1/2}\hat{\Lambda}J(U)\|_{\mathcal{E}_K}^2 \right) \\ &\quad + \left(\|\alpha^{1/2}p^{1/2}\hat{\Theta}^{1/2}\hat{\Lambda}\llbracket U \rrbracket\|_{\Gamma_K}^2 + \|\alpha^{1/2}p^{1/2}\hat{\Theta}^{1/2}\hat{\Lambda}(U - g)\|_{\Sigma_K}^2 \right) \\ &\quad + \left(\|\hat{a}^{1/2}p^{-1}h^{1/2}\hat{\Theta}^{1/2}\hat{\Lambda}\nabla_T \llbracket U \rrbracket\|_{\Gamma_K}^2 + \|\hat{a}^{1/2}p^{-1}h^{1/2}\hat{\Theta}^{1/2}\hat{\Lambda}\nabla_T(U - g)\|_{\Sigma_K}^2 \right). \end{aligned}$$

Here $\mathcal{E}_K = \{e \in \mathcal{E}^{\text{side}} : e \cap \bar{K} \neq \emptyset\}$.

Proof. The proof modifies the argument in [19, Theorem 3.1], which extends the argument for deriving a posteriori error estimates for DG methods in e.g., Karakashian and Pascal [33] and [12]. Let $\tilde{U} \in H^1(\Omega)$ such that $\tilde{U} = g$ on $\partial\Omega$, and

$$\int_{\Omega} a \nabla \tilde{U} \cdot \nabla v dx = \int_{\Omega} a \nabla_h U \cdot \nabla v dx \quad \forall v \in H_0^1(\Omega). \quad (2.21)$$

By the Lax-Milgram lemma, \tilde{U} is well-defined. By the triangle inequality, since $\llbracket u - \tilde{U} \rrbracket = 0$ on $\mathcal{E}^\Gamma \cup \mathcal{E}^{\text{bdy}}$,

$$\begin{aligned} \|u - U\|_{\text{DG}} &\leq \|u - \tilde{U}\|_{\text{DG}} + \|\tilde{U} - U\|_{\text{DG}} \\ &\leq \|a^{1/2}\nabla(u - \tilde{U})\|_{\mathcal{M}} + \|a^{1/2}\nabla_h(U - \tilde{U})\|_{\mathcal{M}} + \|\alpha^{1/2}\llbracket U \rrbracket\|_{\mathcal{E}^\Gamma} + \|p^{-1}h^{1/2}\nabla_T \llbracket U \rrbracket\|_{\mathcal{E}^\Gamma} \\ &\quad + \|\alpha^{1/2}(U - g)\|_{\mathcal{E}^{\text{bdy}}} + \|p^{-1}h^{1/2}\nabla_T(U - g)\|_{\mathcal{E}^{\text{bdy}}}. \end{aligned} \quad (2.22)$$

We now estimate the first two terms in (2.22). We first estimate the conforming component $\|a^{1/2}\nabla(u - \tilde{U})\|_{\mathcal{M}}$. Set $w = u - \tilde{U} \in H_0^1(\Omega)$ and let $w_h = \pi_{hp}w \in \mathbb{X}_p(\mathcal{M})$ be defined in Lemma 2.4. By (2.7) we have

$$\begin{aligned}
(a\nabla(u - \tilde{U}), \nabla w)_{\mathcal{M}} &= (f, w)_{\mathcal{M}} - (a\nabla_h U, \nabla_h w)_{\mathcal{M}} \\
&= (f, w - w_h)_{\mathcal{M}} - (a\nabla_h U, \nabla_h(w - w_h))_{\mathcal{M}} \\
&\quad - (a\nabla_h U, \mathbf{L}(w_h))_{\mathcal{M}} + (a(\mathbf{L}_1(g) - \mathbf{L}(U)), \nabla_h w_h - \mathbf{L}(w_h))_{\mathcal{M}} \\
&\quad + \langle \alpha \llbracket U \rrbracket, \llbracket w_h \rrbracket \rangle_{\mathcal{E}^\Gamma} + \langle p^{-2}h\nabla_T \llbracket U \rrbracket, \nabla_T \llbracket w_h \rrbracket \rangle_{\mathcal{E}^\Gamma} \\
&\quad + \langle \alpha(U - g), w_h \rangle_{\mathcal{E}^{\text{bdy}}} + \langle p^{-2}h\nabla_T(U - g), \nabla_T \llbracket w_h \rrbracket \rangle_{\mathcal{E}^{\text{bdy}}} \\
&:= \mathbf{I}_1 + \cdots + \mathbf{I}_8. \tag{2.23}
\end{aligned}$$

By using integration by parts and the DG magic formula $\llbracket (a\nabla_h U \cdot \mathbf{n})(w - w_h) \rrbracket = \llbracket a\nabla_h U \cdot \mathbf{n} \rrbracket (w - w_h)^+ + (a\nabla_h U \cdot \mathbf{n})^- \llbracket w - w_h \rrbracket$ on any $e \in \mathcal{E}$, we have

$$\mathbf{I}_1 + \mathbf{I}_2 + \mathbf{I}_3 = (R(U), w - w_h)_{\mathcal{M}} - \langle J(U), (w - w_h)^+ \rangle_{\mathcal{E}^{\text{side}}}.$$

Now by using Lemma 2.4, we get

$$|\mathbf{I}_1 + \mathbf{I}_2 + \mathbf{I}_3| \leq C(\|a^{-1/2}(h/p)\Lambda R(U)\|_{\mathcal{M}} + \|\hat{a}^{-1/2}(h/p)^{1/2}\hat{\Lambda}J(U)\|_{\mathcal{E}^{\text{side}}})\|a^{1/2}\nabla w\|_{\mathcal{M}}.$$

Next by the definition of the lifting operators in (2.5)

$$\mathbf{I}_4 = -\langle a(\nabla_h w_h - \mathbf{L}(w_h))^- \cdot \mathbf{n}, \llbracket U \rrbracket \rangle_{\mathcal{E}^\Gamma} + \langle a(\nabla_h w_h - \mathbf{L}(w_h))^- \cdot \mathbf{n}, g - U \rangle_{\mathcal{E}^{\text{bdy}}}.$$

By Lemma 2.3 and Lemma 2.5, we have

$$|\mathbf{I}_4| \leq C(\|\alpha^{1/2}\zeta \llbracket U \rrbracket\|_{\mathcal{E}^\Gamma} + \|\alpha^{1/2}\zeta(U - g)\|_{\mathcal{E}^{\text{bdy}}})\|a^{1/2}\nabla w\|_{\mathcal{M}}.$$

The other terms can be estimated similarly

$$\begin{aligned}
|\mathbf{I}_5 + \cdots + \mathbf{I}_8| &\leq C(\|\alpha^{1/2}\zeta \llbracket U \rrbracket\|_{\mathcal{E}^\Gamma} + \|\alpha^{1/2}\zeta(U - g)\|_{\mathcal{E}^{\text{bdy}}})\|a^{1/2}\nabla w\|_{\mathcal{M}} \\
&\quad + C\|\hat{a}^{1/2}p^{-1}h^{1/2}\hat{\Theta}^{1/2}\hat{\Lambda}\nabla_T \llbracket U \rrbracket\|_{\mathcal{E}^\Gamma}\|a^{1/2}\nabla w\|_{\mathcal{M}} \\
&\quad + C\|\hat{a}^{1/2}p^{-1}h^{1/2}\hat{\Theta}^{1/2}\hat{\Lambda}\nabla_T(U - g)\|_{\mathcal{E}^{\text{bdy}}}\|a^{1/2}\nabla w\|_{\mathcal{M}}.
\end{aligned}$$

Substituting the estimates for $\mathbf{I}_1, \dots, \mathbf{I}_8$ into (2.23), we obtain

$$\|a^{1/2}\nabla(u - \tilde{U})\|_{\mathcal{M}} \leq C \left(\sum_{K \in \mathcal{M}} \xi_K^2 \right)^{1/2}. \tag{2.24}$$

The nonconforming component $\|a^{1/2}\nabla_h(U - \tilde{U})\|_{\mathcal{M}}$ can be estimated by the same argument as that in [19, Theorem 3.1] to obtain

$$\begin{aligned}
\|a^{1/2}\nabla_h(U - \tilde{U})\|_{\mathcal{M}} &\leq C(\|\hat{a}^{1/2}ph^{-1/2}\llbracket U \rrbracket\|_{\mathcal{E}^\Gamma} + \|\hat{a}^{1/2}p^{-1}h\nabla_T \llbracket U \rrbracket\|_{\mathcal{E}^\Gamma}) \\
&\quad + C(\|\hat{a}^{1/2}ph^{-1/2}(U - g)\|_{\mathcal{E}^{\text{bdy}}} + \|\hat{a}^{1/2}p^{-1}h^{1/2}\nabla_T(u - g)\|_{\mathcal{E}^{\text{bdy}}}).
\end{aligned}$$

This, together with (2.22) and (2.24), completes the proof. \square

We remark that in above proof $\mathbf{L}(w_h) \neq 0$, which is different from the proof in [19, Theorem 3.1] where $\mathbf{L}(w_h) = 0$ due to the unfitted finite element space being $\mathbb{H}_p(\mathcal{M})$ and the domain being assumed to be a union of rectangles so that $\pi_{hp}w$ can be chosen in $\mathbb{H}_p(\mathcal{M}) \cap H_0^1(\Omega)$.

The lower bound of the a posteriori error estimator ξ_K can also be established by the similar argument as that in [19, Theorem 4.1]. We leave it to the interested readers.

3 The merging algorithm

In this section, we propose the merging algorithm to generate the induced mesh for the piecewise smooth interface and boundary. A reliable algorithm to generate the induced mesh is developed in [20, Algorithm 6] for arbitrarily shaped C^2 -smooth interfaces. The algorithm is based on the concept of the admissible chain of interface elements, the classification of patterns for merging elements, and appropriate ordering in generating macro-elements. Our strategy to treat the piecewise smooth interface or boundary is first to design singular patterns that are large macro-elements surrounding each singular point of the interface or boundary, then use [20, Algorithm 6] to deal with the remaining interface or boundary elements inside which the interface or boundary is C^2 -smooth.

We now recall some notation from [20]. A chain of interface or boundary elements $\mathfrak{C} = \{G_1 \rightarrow G_2 \rightarrow \cdots \rightarrow G_n\}$ orderly consists of n interface or boundary elements $G_i \in \mathcal{T}^\Gamma$ or $G_i \in \mathcal{T}^\Sigma$, $i = 1, \dots, n$, such that $\bar{\Gamma}_{G_i} \cup \bar{\Gamma}_{G_{i+1}}$ is a continuous curve, $1 \leq i \leq n-1$. We call n the length of \mathfrak{C} and denote $\mathfrak{C}\{i\} = G_i$, $i = 1, \dots, n$.

For any $K \in \mathcal{T}$, we call $N(K) \in \mathcal{T}$ a neighboring element of K if K and $N(K)$ share a common side. Set $\mathcal{S}(K)_0 = \{K\}$, and for $j \geq 1$, denote $\mathcal{S}(K)_j = \{K'' \in \mathcal{T} : \exists K' \in \mathcal{S}(K)_{j-1} \text{ such that } \bar{K}'' \cap \bar{K}' \neq \emptyset\}$, that is, $\mathcal{S}(K)_j$ is the set of all k -th layer elements surrounding K , $0 \leq k \leq j$. Obviously, $\mathcal{S}(K)_0 \subset \mathcal{S}(K)_1 \subset \cdots \subset \mathcal{S}(K)_j$ for any $j \geq 1$.

The following definition of the admissible chain is introduced in [20] for interface elements. We include here also for the boundary elements.

Definiton 3.1. *A chain of interface or boundary elements \mathfrak{C} is called admissible if the following rules are satisfied.*

1. *For any $K \in \mathfrak{C}$, all elements in $\mathcal{S}(K)_2$ have the same size as that of K .*
2. *If $K \in \mathfrak{C}$ has a side e such that $\bar{e} \subset \Omega_i$, then e must be a side of some neighboring element $N(K) \subset \Omega_i$, $i = 1, 2$.*
3. *Any elements $K \in \mathcal{T} \setminus \mathcal{T}^\Gamma \cup \mathcal{T}^\Sigma$ can be neighboring at most two elements in \mathfrak{C} .*
4. *For any $K \subset \Omega_i$, the interface or boundary elements in $\mathcal{S}(K)_j$, $j = 1, 2$, must be connected in the sense that the interior of the closed set $\cup\{\bar{G} : G \in \mathcal{S}(K)_j \cap \mathcal{T}^\Gamma\}$ or $\cup\{\bar{G} : G \in \mathcal{S}(K)_j \cap \mathcal{T}^\Sigma\}$ is a connected domain.*

Notice that for the smooth interface or boundary, only type $\mathcal{T}_1, \mathcal{T}_2$ elements occur in the admissible chain, the following theorem is proved in [20, Theorem 3.1] for the admissible chain of interface elements whose start and end elements are of type \mathcal{T}_2 elements. A closer check of the proof reveals that the conclusion also holds when the start or end elements are two neighboring type \mathcal{T}_1 elements. The extension of the theorem to the chain of boundary elements is straightforward. Here we omit the details.

Theorem 3.1. *Let $\delta_0 \in (0, 1/5]$. For any admissible chain of interface or boundary elements \mathfrak{C} with length $n \geq 2$, if the start elements of \mathfrak{C} satisfy $\mathfrak{C}(1) \in \mathcal{T}_2$ or $\mathfrak{C}(1), \mathfrak{C}(2) \in \mathcal{T}_1$ and the end elements of \mathfrak{C} also satisfy $\mathfrak{C}(n) \in \mathcal{T}_2$ or $\mathfrak{C}(n-1), \mathfrak{C}(n) \in \mathcal{T}_1$, then the merging algorithm in [20, Algorithm 6] can successfully generate a locally induced mesh with input \mathfrak{C} .*

Here and in the following, we call a locally induced mesh of a chain \mathfrak{C} if it is a union of large elements that covers the interface or boundary included in the elements in \mathfrak{C} .

3.1 The singular pattern

We start by introducing the definition of the singular pattern.

Definiton 3.2. *For each singular element $K \in \mathcal{T}$, there exists a macro-element $M(K)$ that is a union of elements surrounding K such that $M(K)$ is a large element. Moreover, if $G_1, G_2 \in \mathcal{T}$ are two interface or boundary elements in $\mathcal{S}(M(K))_1 \setminus M(K)$, then for $i = 1, 2$, either $G_i \in \mathcal{T}_2$ or $G_i \in \mathcal{T}_1$ in which case there is a neighboring element $G'_i \in \mathcal{T}_1$ in $\mathcal{S}(M(K))_1 \setminus M(K)$. Denote $\mathcal{P}_i = \{G_i\}$ if $G_i \in \mathcal{T}_2$ or $\mathcal{P}_i = \{G_i, G'_i\}$ if $G_i \in \mathcal{T}_1$. We assume $\text{dist}(\mathcal{P}_1, \mathcal{P}_2) \geq 2$, where $\text{dist}(\mathcal{P}_1, \mathcal{P}_2)$ is the minimum number of non-interface or non-boundary elements in $\mathcal{S}(M(K))_1 \setminus M(K)$ connecting $\mathcal{P}_1, \mathcal{P}_2$, see Fig.3.1. We call $M(K)$ the singular pattern including K and $\mathcal{P}_1, \mathcal{P}_2$ the outlet patches of the macro-element $M(K)$.*

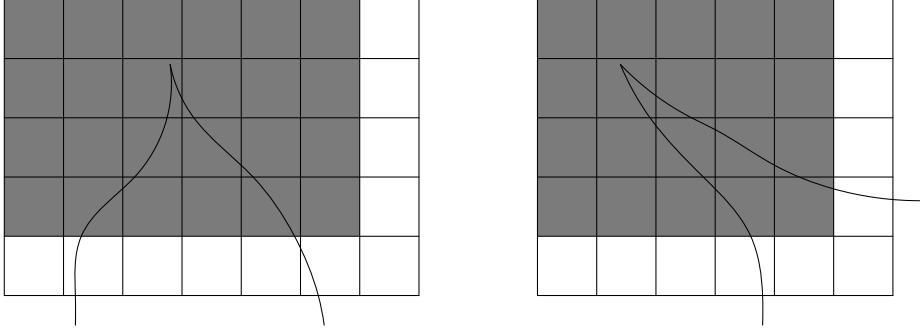


Figure 3.1: Examples of the singular pattern.

We recall that $\mathcal{S}(M(K))_1 \setminus M(K)$ is the union of the first layer elements in \mathcal{T} surrounding $M(K)$. The assumptions on the patch of elements $\mathcal{P}_1, \mathcal{P}_2$ are important for us to use [20, Algorithm 6] to construct macro-elements for all remaining elements in \mathcal{T}^Γ or \mathcal{T}^Σ inside which the interface or boundary is C^2 smooth.

Since for each singular element K , $K_i = K \cap \Omega_i$, $i = 1, 2$, is locally a curved sector, the following lemma indicates that one can always construct a singular pattern $M(K)$ if the mesh is locally refined around each singular point.

Lemma 3.1. *Let S be a sector bounded by two half lines L_1, L_2 with vertex $Q \in K$, $K \in \mathcal{T}$. Then there exists a rectangular macro-element $M(K)$ that is a large element and for $i = 1, 2$, $\mathcal{P}_i = \{K' \in \mathcal{T} : K' \subset \mathcal{S}(M(K))_1 \setminus M(K), K' \cap L_i \neq \emptyset\}$ includes either one \mathcal{T}_2 element or two neighboring \mathcal{T}_1 elements. Moreover, $\text{dist}(\mathcal{P}_1, \mathcal{P}_2) \geq 2$ and the element singular index $\tilde{\delta}_{M(K)}$ is independent of the element size h_K .*

Proof. Let h_1, h_2 be the length of the horizontal and vertical sides of K , respectively. Let $Q = (-\alpha h_1, \beta h_2)$, $\alpha, \beta \in (0, 1)$, be the vertex of the sector S , and for $i = 1, 2$, the equation of L_i is $x_2 - \beta h_2 = k_i(x_1 + \alpha h_1)$ with the convention that if $k_i = \infty$, the equation is $x_1 + \alpha h_1 = 0$. It is clear that if $|k_i| < h_2/h_1$, L_i tends to the infinity in the region I, III

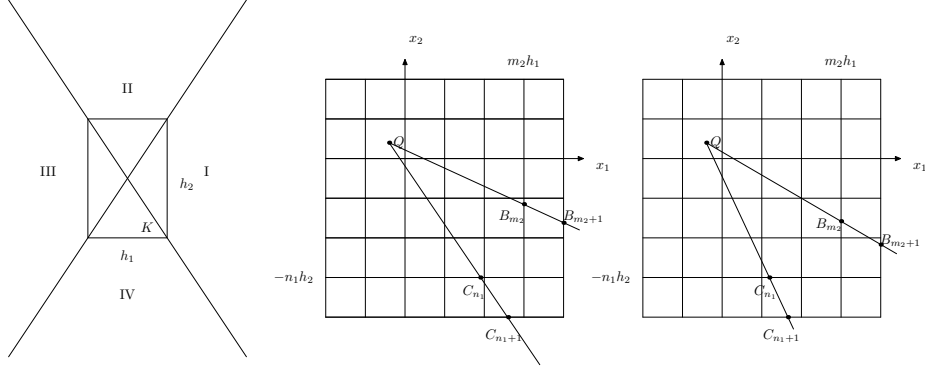


Figure 3.2: The figures used in the proof of Lemma 3.1.

marked in Fig.3.2(left), and if $|k_i| > h_2/h_1$, L_i tends to the infinity in the region II, IV in Fig.3.2(left). Let $M(K) = (-m_1h_1, m_2h_1) \times (-n_1h_2, n_2h_2)$, $m_i, n_i \in \mathbb{N}$, $i = 1, 2$, be the macro-element.

In the following, we prove the lemma when $|k_1| \leq h_2/h_1, |k_2| > h_2/h_1$. We first assume $k_1, k_2 < 0$ so that $\lambda_1 := k_1h_1/h_2 \in (-1, 0)$, $\lambda_2 := k_2^{-1}h_2/h_1 \in (-1, 0)$. Let $m_1 = 2, n_2 = 2$ in the macro-element $M(K)$, see Fig.3.2(middle) and Fig.3.2(right). Denote by $B_{m_2} = (m_2h_1, b_{m_2}), B_{m_2+1} = ((m_2 + 1)h_1, b_{m_2+1})$ the intersection points of L_1 with the lines $x_1 = m_2h_1, x_1 = (m_2 + 1)h_1$, and $C_{n_1} = (c_{n_1}, -n_1h_2), C_{n_1+1} = (c_{n_1+1}, -(n_1 + 1)h_2)$ the intersection points of L_2 with the lines $x_2 = -n_1h_2, x_2 = -(n_1 + 1)h_2$. Obviously, $b_{m_2} - b_{m_2+1} = -k_1h_1 \leq h_2$, which implies that L_1 intersects $\mathcal{S}(M(K))_1 \setminus M(K)$ either with one \mathcal{T}_2 element or two neighboring \mathcal{T}_1 elements. Similarly, L_2 intersects $\mathcal{S}(M(K))_1 \setminus M(K)$ with either one \mathcal{T}_2 element or two neighboring \mathcal{T}_1 elements.

In order to guarantee that $\text{dist}(\mathcal{P}_1, \mathcal{P}_2) \geq 2$, we require $b_{m_2+1} \geq -(n_1 - 1)h_2, c_{n_1} < (m_2 - 1)h_2$ in the case of Fig.3.2(middle) or $b_{m_2} \geq -(n_1 - 1)h_2, c_{n_1+1} \leq (m_2 - 1)h_1$ in the case of Fig.3.2(right). In the case shown in Fig.3.2(middle), it is easy to see that $b_{m_2+1} \geq -(n_1 - 1)h_2, c_{n_1} < (m_2 - 1)h_2$ is equivalent to $-\lambda_1(m_2 + 1 + \alpha) \leq n_1 + \beta - 1$, $-\lambda_2(n_1 + \beta) < m_2 + \alpha - 1$, which implies $n_1 + \beta \geq (1 - 2\lambda_1)/(1 - \lambda_1\lambda_2), m_2 + \alpha + 1 > (2 - \lambda_2)/(1 - \lambda_1\lambda_2)$. Thus one can choose

$$m_2 = \left\lfloor \frac{2 - \lambda_2}{1 - \lambda_1\lambda_2} \right\rfloor, \quad n_1 = \left\lfloor \frac{1 - 2\lambda_1}{1 - \lambda_1\lambda_2} \right\rfloor + 1$$

to guarantee $\text{dist}(\mathcal{P}_1, \mathcal{P}_2) \geq 2$, where for any $\gamma \in \mathbb{R}$, $\lfloor \gamma \rfloor$ is the integer strictly less than γ . Similarly, in the case displayed in Fig.3.2(right), one can take

$$m_2 = \left\lfloor \frac{1 - 2\lambda_2}{1 - \lambda_1\lambda_2} \right\rfloor + 1, \quad n_1 = \left\lfloor \frac{2 - \lambda_1}{1 - \lambda_1\lambda_2} \right\rfloor$$

to guarantee $\text{dist}(\mathcal{P}_1, \mathcal{P}_2) \geq 2$. This shows the lemma when $k_1, k_2 < 0$. The other cases when either one of k_1, k_2 or both k_1, k_2 are non-negative can be proved analogously. In fact, if $k_1 \geq 0, k_2 \geq 0$, then $m_1 = \lfloor 2\lambda_2 \rfloor + 2, m_2 = 1, n_1 = 1, n_2 = \lfloor 2\lambda_1 \rfloor + 3$; if $k_1 \geq 0, k_2 < 0$, then $m_1 = 2, m_2 = \lfloor 2(-\lambda_2)^+ \rfloor + 2, n_1 = 1, n_2 = \lfloor (m_2 + 1)\lambda_1 \rfloor + 3$; and if $k_1 < 0, k_2 \geq 0$, then $m_1 = \lfloor (n_1 + 1)\lambda_2 \rfloor + 2, m_2 = 1, n_1 = \lfloor 2(-\lambda_1)^+ \rfloor + 2, n_2 = 2$.

The macro-element is a large element with $\delta_{M(K)}, \tilde{\delta}_{M(K)} \geq \min(1/(m_1 + m_2), 1/(n_1 + n_2))$ by Definition 2.2 of large elements. We note that $m_i, n_i, i = 1, 2$, are fixed constants, which depend only on the angle of the sector S at vertex but are independent of h_K . This completes the proof when $|k_1| \leq h_2/h_1, |k_2| > h_2/h_1$.

For the other cases, we just give the macro-element $M(K)$ and omit the details of the proof. By the symmetry, we only need to consider two cases. The first is when L_1, L_2 tend to infinity in the same region, for example in the region IV. Then $|k_i| > h_2/h_1, i = 1, 2$, so that $\lambda_i = k_i^{-1}h_2/h_1$ satisfies $|\lambda_i| < 1, i = 1, 2$. The integers $m_i, n_i, i = 1, 2$, in the macro-element $M(K)$ are defined by

$$m_1 = \max_{i=1,2} \lfloor (n_1 + 1)\lambda_i^+ \rfloor + 3, \quad m_2 = \max_{i=1,2} \lfloor (n_1 + 1)(-\lambda_i)^+ \rfloor + 2,$$

$$n_1 = \left\lfloor \frac{3}{|\lambda_1 - \lambda_2|} \right\rfloor + 1, \quad n_2 = 2.$$

It is clear that $M(K)$ is a large element with $\delta_{M(K)}, \tilde{\delta}_{M(K)} \geq \min(1/(m_1 + m_2), 1/(n_1 + n_2))$.

The second case is when L_1 and L_2 tend to infinity in the opposite regions, for example, L_1 in the region II and L_2 in the region IV. Then the integers $m_i, n_i, i = 1, 2$, in the macro-element $M(K)$ are defined by

$$m_1 = \max_{i=1,2} \lfloor 2\lambda_i^+ \rfloor + 3, \quad m_2 = \max_{i=1,2} \lfloor 2(-\lambda_i)^+ \rfloor + 2, \quad n_1 = 1, \quad n_2 = 2.$$

It is obvious that $M(K)$ is a large element with $\delta_{M(K)}, \tilde{\delta}_{M(K)} \geq \min(1/(m_1 + m_2), 1/(n_1 + n_2))$. \square

Notice that the macro-element $M(K)$ constructed in Lemma 3.1 is associated with the mesh \mathcal{T} . The following lemma shows that the macro-element constructed is also nested with respect to the quad-refinements of the mesh. This fact is important for us to construct admissible subchains of interface or boundary elements inside which the interface or boundary is smooth. The proof is rather straightforward and we omit the details.

Lemma 3.2. *Let S be a sector bounded by two half lines L_1, L_2 with vertex $Q \in K, K \in \mathcal{T}$. Let $M(K)$ be the macro-element constructed in Lemma 3.1. If one refines all elements in $M(K)$ by quad refinement to obtain a new mesh \mathcal{T}' and $K' \in \mathcal{T}'$ is the singular element containing Q , then the macro-element $M(K')$ constructed on the mesh \mathcal{T}' satisfies $M(K') \subset M(K)$ and the element singular index $\tilde{\delta}_{M(K')}(\mathcal{T}') = \tilde{\delta}_{M(K)}(\mathcal{T})$. Moreover, the interface or boundary elements of \mathcal{T}' included in $M(K) \setminus M(K')$ consist of either \mathcal{T}_2 or two neighboring \mathcal{T}_1 elements and thus can be merged to generate large elements over the mesh \mathcal{T}' inside $M(K)$, see Fig.3.3.*

An important property of the singular pattern is that it stays unchanged if its outlet patch requires refinement due to the refinement of its neighboring elements in the chain of elements connecting to another singular pattern. Let \mathcal{P} be an outlet patch of $M(K)$ that is connected to another singular pattern by a chain \mathfrak{G} . If the neighboring elements of \mathcal{P} in the chain \mathfrak{G} are refined, one can quad-refine the elements in \mathcal{P} and their neighboring elements in $\mathcal{S}(M(K))_1$ so that the interface or boundary in \mathcal{P} can be covered by two large elements M_1, M_2 , see Fig.3.3. If the neighboring elements of \mathcal{P} in \mathfrak{G} are further refined, one needs only

to quad-refine the elements in M_2 and possibly their neighboring elements inside $\mathcal{S}(M(K))_1$ so that the interface or boundary inside \mathcal{P} can be covered by large elements M_1, M_{21}, M_{22} . This process of refining the outlet patches can be continued until the elements in the chain \mathcal{G} are constructed by [20, Algorithm 6]. We summarized the algorithm for refining the outlet patch \mathcal{P} as the following algorithm. In the following, we define the level of the element $L(K) = 0 \forall K \in \mathcal{T}_0$. When $K \in \mathcal{T}$ is refined by quad refinement to four sub-elements K_i , we set $L(K_i) = L(K) + 1, i = 1, 2, 3, 4$. Then we can use the level of an element to denote the size of the element.

Algorithm 1: The algorithm for refining an outlet patch.

Input: A singular pattern $M(K)$, an outlet patch \mathcal{P} , and the difference of the level of elements $\ell = L(K') - L(K''), K' \in \mathcal{P}, K'' \in (\mathcal{M}^\Gamma \cup \mathcal{M}^\Sigma) \setminus M(K)$ neighboring to K' .

Output: The refined outlet patch \mathcal{P}' and a set of large elements $\mathcal{L}(K)$ covering the interface or boundary elements inside $\mathcal{P} \setminus \mathcal{P}'$.

1° Set $i = 1, \mathcal{P}_1 = \mathcal{P}$.

2° For $i = 1, \dots, \ell$, do

(i) Quad-refine elements in \mathcal{P}_i and their neighboring elements inside $\mathcal{S}(M(K))_1 \setminus M(K)$, which are not merged yet, to generate a new mesh, set \mathcal{P}_{i+1} as the set of interface or boundary elements neighboring $\partial\mathcal{S}(M(K))_1$.

(ii) Merge the interface or boundary elements in $\mathcal{P}_i \setminus \mathcal{P}_{i+1}$ with their neighboring elements to generate a large element M . Add M to $\mathcal{L}(K)$.

3° Set $\mathcal{P}' = \mathcal{P}_{\ell+1}$.

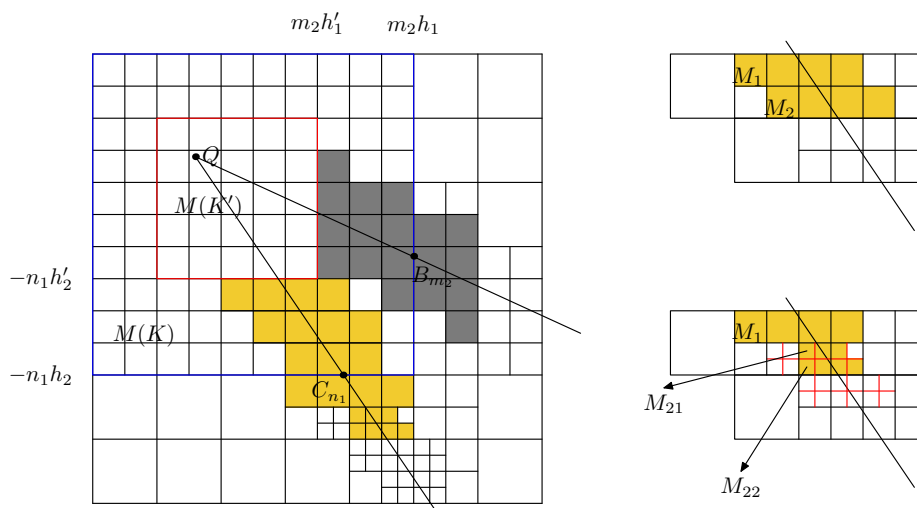


Figure 3.3: The refinement of a singular pattern and its outlet patch, where $h'_i = h_i/2, i = 1, 2$. The macro-element $M(K') = (-2h'_1, m_2h'_1) \times (-n_1h'_2, 2h_2)$, $M(K) = (-2h_1, m_2h_1) \times (-n_1h_2, 2h_2)$.

We formulate the process in the following algorithm for refining a singular pattern if its outlet patch \mathcal{P} is refined.

Algorithm 2: The merging algorithm for refining a singular pattern.

Input: A singular pattern $M(K)$.

Output: A locally refined mesh over $M(K)$ and a set of large elements $\mathcal{L}(K)$ covering the interface or boundary inside $M(K)$.

1° Quad-refine elements in $M(K)$ to obtain a new mesh, find the singular element K' on the new mesh, construct the singular pattern $M(K')$.

2° Merge the elements to generate large elements $N_i, i = 1, \dots, n_K$, which cover the boundary or interface inside $M(K) \setminus M(K')$. Add $M(K')$ and $N_i, i = 1, \dots, n_K$, to $\mathcal{L}(K)$.

3.2 The merging algorithm

After dealing with the singular elements, the remaining interface or boundary elements consist of several chains of elements inside which the interface or boundary is C^2 -smooth. Let \mathfrak{G} be a chain of interface or boundary elements connecting two singular patterns $M(K_s), M(K_e)$ with the associated outlet patch $\mathcal{P}_s, \mathcal{P}_e$, respectively. By definition, the start patch \mathcal{P}_s and the end patch \mathcal{P}_e are one of $\mathcal{P}_i, i = 1, 2$, where $\mathcal{P}_1 = \{G\}, G \in \mathcal{T}_2$, and $\mathcal{P}_2 = \{G_1, G_2\}, G_1, G_2 \in \mathcal{T}_1$.

One way to construct a locally induced mesh of \mathfrak{G} is to refine the elements in $\mathcal{S}(K)_2, K \in \mathfrak{G}$, to a uniform size so that the refined interface or boundary elements consist of an admissible chain \mathfrak{G}' and thus one can use the merging algorithm in [20, Algorithm 6]. However, it may do too many extra refinements to be suitable for the adaptive finite element algorithm. Our approach is to construct admissible subchains of \mathfrak{G} with possible different element sizes in different subchains. In addition, the start and end patch of each admissible subchain belong to $\mathcal{P}_1, \mathcal{P}_2$ so that [20, Algorithm 6] can be used to generate the locally induced meshes of the subchain.

For a given chain \mathfrak{G} , let $\mathcal{G} \in \mathbb{R}^{n_a \times 2}$ be a two-dimensional array so that for $i = 1, \dots, n_a$, $\mathcal{G}(i, 1), \mathcal{G}(i, 2)$ are the index of the start and end element of the i th admissible subchain in \mathfrak{G} . We use the following algorithm to find \mathcal{G} .

Algorithm 3: Find all admissible subchains connecting two singular patterns $M(K_s), M(K_e)$.

Input: A chain \mathfrak{G} that connects singular patterns $M(K_s), M(K_e)$ associated with outlet patches $\mathcal{P}_s, \mathcal{P}_e$, respectively.

Output: An updated chain \mathfrak{G} consisting of admissible subchains covering the interface or boundary inside the elements in \mathfrak{G} , and an index matrix $\mathcal{G} \in \mathbb{R}^{n_a \times 2}$ of admissible subchains of \mathfrak{G} .

1° Locally refine the elements in \mathfrak{G} such that \mathfrak{G} satisfies the rules 2, 3, 4 in Definition 3.1. During the refining processes, call the refinement procedure in [12, §6] such that the mesh satisfies Assumption (H3). If the outlet patch \mathcal{P}_s or \mathcal{P}_e need to be refined then call Algorithm 1. Set $i_s = 1, n_a = 0$.

2° Find the maximum number i_e such that $\mathfrak{G}(i_s : i_e)$ have the same size.

3° **if** $\mathfrak{G}(i_e) == \mathfrak{G}(end)$ **then**

Set $n_a = n_a + 1$ and $\mathcal{G}(n_a, 1 : 2) = [i_s, i_e]$.

```

    RETURN  $\mathcal{G}$  and  $\mathfrak{G}$ .
  end
4° if  $|L(\mathfrak{G}(i_e + 1)) - L(\mathfrak{G}(i_e))| \leq 2$  then
  if  $(\mathfrak{G}(i_e) \in \mathcal{P}_1$  or  $\mathfrak{G}(i_e - 1 : i_e) \in \mathcal{P}_2)$ 
    and  $(\mathfrak{G}(i_e + 1) \in \mathcal{P}_1$  or  $\mathfrak{G}(i_e + 1 : i_e + 2) \in \mathcal{P}_2)$  then
    Set  $n_a = n_a + 1$ ,  $\mathcal{G}(n_a, 1 : 2) = [i_s, i_e]$ ,  $i_s = i_e + 1$  and GOTO 2°.
  end
else
  if  $L(\mathfrak{G}(i_e + 1)) < L(\mathfrak{G}(i_e))$  then
    if  $\mathfrak{G}(i_e + 1) \in \mathcal{P}_e$  then
      Call Algorithm 1 to refine  $\mathcal{P}_e$  to get  $\mathcal{P}'_e$ , set  $\mathcal{P}_e = \mathcal{P}'_e$  and update the  $\mathfrak{G}$  as a
      chain which connecting to  $\mathcal{P}_s$  and  $\mathcal{P}_e$ . GOTO 2°.
    else Refine  $\mathfrak{G}(i_e + 1)$ , GOTO 2°.
    end
  else
    if  $\mathfrak{G}(i_e) \in \mathcal{P}_s$  then
      Call Algorithm 1 to refine  $\mathcal{P}_s$  to get  $\mathcal{P}'_s$ , set  $\mathcal{P}_s = \mathcal{P}'_s$  and update the  $\mathfrak{G}$  as a
      chain which connecting to  $\mathcal{P}_s$  and  $\mathcal{P}_e$ . GOTO 2°.
    else
      Refine  $\mathfrak{G}(i_e)$ 
      if  $i_s == i_e$  then
        Set  $i_s = \mathcal{G}(n_a, 1)$  and remove the  $n_a$ -th row of  $\mathcal{G}$ ,  $n_a = n_a - 1$ .
      end
      GOTO 2°.
    end
  end
end
end
end

```

We remark that in the worst case, when all elements in \mathfrak{G} are refined to be of the same size to consist of an admissible chain, Algorithm 3 will return one admissible chain, that is, $\mathcal{G} = [1, \text{length}(\mathfrak{G})]$.

Our final merging algorithm combines the singular patterns and Algorithm 3 of finding admissible subchains to obtain an induced mesh whose elements cover the interface or boundary.

Algorithm 4: The merging algorithm for a closed chain \mathfrak{C} .

Input: A closed chain \mathfrak{C} .

Output: The induced mesh $\text{Induced}(\mathcal{T})$.

1° Construct the singular patterns for each singular element, then the remainder interface or boundary elements will consist of some chains, each chain \mathfrak{G} satisfying $\mathfrak{G}(1) \in \mathcal{P}_1$ or $\mathfrak{G}(1 : 2) \in \mathcal{P}_2$ and $\mathfrak{G}(\text{end}) \in \mathcal{P}_1$ or $\mathfrak{G}(\text{end} - 1 : \text{end}) \in \mathcal{P}_2$.

2° For each remainder chain \mathfrak{G} , call Algorithm 3 with input \mathfrak{G} to obtain the index matrix $\mathcal{G} \in \mathbb{R}^{n_a \times 2}$.

3° For each index matrix, call [20, Algorithm 6] with input $\mathfrak{G}(\mathcal{G}(i, 1) : \mathcal{G}(i, 2))$, $i = 1, \dots, n_a$, to generate the locally induced mesh.

4° Construct new singular patterns by Algorithm 2 whose outlet patches are refined in steps 2°.

From the definition of the singular patterns and the Theorem 3.1, the above algorithm will successfully generate the induced mesh for the arbitrarily shaped piecewise smooth interface or boundary. Thus we have the following theorem.

Theorem 3.2. *Let $\delta_0 = \min(1/5, \delta_s)$, where δ_s is the minimum element singular index of all singular elements. For any closed chain of interface or boundary elements \mathfrak{C} , Algorithm 4 will generate an induced mesh whose elements cover the interface or boundary included in the elements in \mathfrak{C} .*

4 Numerical examples

In this section, we present some numerical examples to confirm our theoretical results. We use a posteriori error estimator in Theorem 2.1 to design the adaptive algorithm combined with our mesh merging algorithm. The hierarchical shape functions in Szabó and Babuška [41, §5.3.2] are used on quadrilateral elements. For shape functions on triangular elements, we refer to Adjerid et al. [1] where the orthogonalization is applied to the face shape functions to reduce the condition number of the stiffness matrix. The hanging nodes are treated by modifying the connectivity mapping in Ainsworth and Senior [2], in which they provide the efficient realization on non-uniform Cartesian meshes.

The generic form of our adaptive unfitted finite element method is given below.

Algorithm 5: General form of an adaptive unfitted finite element method.

Given a tolerance $TOL > 0$, the steering parameters $\eta_0 \in (0, 1/2)$, $\gamma \in (0, 1)$, and an initial Cartesian mesh \mathcal{T}_0 . Set $\ell = 0$ and do

- (1) Let the interface and boundary elements of \mathcal{T}_ℓ form two chains \mathfrak{C} and \mathfrak{C}' , respectively. Call the refinement procedure in [12, §6] such that \mathcal{T}_ℓ satisfies Assumption (H3). Use merging Algorithm 4 to generate an induced mesh $\mathcal{M}_\ell = \text{Induced}(\mathcal{T}_\ell)$.
- (2) If the interface or boundary elements in \mathcal{M}_ℓ do not satisfy Assumption (H2), set $S = \{K' \in \mathcal{T}_\ell : K' \subset K, \eta_{K'} > \eta_0 \text{ for some } K \in \mathcal{M}_\ell\}$, release all merged elements in \mathfrak{C} or \mathfrak{C}' , refine elements in S by quad refinements, **GOTO** (1).
- (3) Compute the unfitted finite element solution U_ℓ satisfying (2.6) on the mesh \mathcal{M}_ℓ .
- (4) Compute the a posteriori error indicators $\xi_K \forall K \in \mathcal{M}_\ell$ and the global (a posteriori) error estimator $\mathcal{E}(U_\ell, \mathcal{M}_\ell) = (\sum_{K \in \mathcal{M}_\ell} \xi_K^2)^{1/2}$.
- (5) If $\frac{\mathcal{E}(U_\ell, \mathcal{M}_\ell)}{\mathcal{E}(U_0, \mathcal{M}_0)} < TOL$ then **STOP**.
- (6) Mark the elements in $\widehat{\mathcal{M}}_\ell \subset \mathcal{M}_\ell$ such that

$$\left(\sum_{K \in \widehat{\mathcal{M}}_\ell} \xi_K^2 \right)^{1/2} \geq \gamma \mathcal{E}(U_\ell, \mathcal{M}_\ell).$$

- (7) Refine the elements in $\widehat{\mathcal{T}}_\ell = \{K \in \mathcal{T}_\ell : \overline{K} \cap \overline{K'} \neq \emptyset, K' \in \widehat{\mathcal{M}}_\ell\}$ to obtain $\mathcal{T}_{\ell+1}$.

(8) Set $\ell = \ell + 1$, and **GOTO** (1).

In the following examples, we set $\eta_0 = 0.05$ and $\gamma = 0.5$, unless otherwise stated. The algorithms are implemented in MATLAB on a workstation with Intel(R) Core(TM) i9-10885H CPU 2.40GHz and 64GB memory.

Example 1. Let $\Omega = \{(x_1, x_2) : (\xi - \frac{1}{2})^2 + \eta^2 < 1, (\xi + \frac{1}{2})^2 + \eta^2 < 1\}$, where $\xi = \cos(\theta)x_1 + \sin(\theta)x_2$, $\eta = -\sin(\theta)x_1 + \cos(\theta)x_2$, and $\theta = \frac{2\pi}{5}$. The boundary of the domain has two singular points at $A = (-\frac{\sqrt{3}}{2}\sin(\theta), \frac{\sqrt{3}}{2}\cos(\theta))$, $B = (\frac{\sqrt{3}}{2}\sin(\theta), -\frac{\sqrt{3}}{2}\cos(\theta))$, see Fig.4.1(a). Let the coefficient $a = 1$ in Ω , the source f and boundary condition g be given such that the exact solution is

$$u_1(x_1, x_2) = \frac{1}{\sqrt{2}}\Re[(z^2 + 3/4)^{1/2}], \quad \text{or} \quad u_2(x_1, x_2) = \frac{1}{\sqrt{2}}\Re[(z^2 + 3/4)^{1/2}] + \cos(20x_1x_2),$$

where $z = \xi + \mathbf{i}\eta$ and $\Re[w]$ denotes the real part of w . We choose the negative half real line in the complex plane as the branch cut of $z^{1/2}$. Notice that $(z^2 + 3/4)^{1/2}$ is analytic in Ω but has singularities at A, B . Thus $\Re[(z^2 + 3/4)^{1/2}]$ is harmonic in Ω but is singular at A, B .

Fig.4.2(a) shows the decay of the error $\|u_1 - U_\ell\|_{\text{DG}}$ for $p = 1, 2, 3, 4, 5$, which is faster than the quasi-optimal decay $CN_\ell^{-\frac{p}{2}}$ for high-order methods. Here N_ℓ is the number of the degrees of freedom (#DoFs) of the mesh \mathcal{M}_ℓ . This is because the exact solution u_1 is very smooth except at A, B . The error of high-order methods in the smooth region is much smaller than the error in the region near A, B . The adaptive algorithm always refines elements close to A, B . The asymptotic behavior of the quasi-optimal decay of the high-order methods has not been reached before the code stops when the element size near the singularity is less than 10^{-9} . However, Fig.4.3 (a) shows the quasi-optimal decay of the error $\|u_2 - U_\ell\|_{\text{DG}} \approx CN_\ell^{-p/2}$ when the solution u_2 has high frequency structures. Table 1 shows clearly that the error of high-order methods is much smaller than the low-order method when the #DoFs are almost the same. Fig.4.4 shows the computational meshes for $p = 1, 3, 5$ with almost the same #DoFs.

Fig.4.2(b) and Fig.4.3(b) depict the effectivity index

$$I_{\text{eff}} = \mathcal{E}(U_\ell, \mathcal{M}_\ell) / \|u - U_\ell\|_{\text{DG}},$$

which ranges in (3.5, 7.5). It shows that our a posteriori error estimates can effectively estimate the errors of the numerical solutions.

	$p = 1$	$p = 3$	$p = 5$
#DoFs	52757	51205	51891
Error	4.51E-02	7.12E-03	1.29E-05

Table 1: Example 1: The error of the numerical solutions and #DoFs when the exact solution is u_2 .

Example 2. We consider a five-star shaped singular interface problem, see Fig.4.1 (right). Let $\Omega_1 = \{(r \cos(\theta), r \sin(\theta)) : r < q(\theta), \theta \in [\frac{\pi}{10}, \frac{21\pi}{10}]\}$ and $\Omega_2 = (-2, 2)^2 \setminus \bar{\Omega}_1$, where

$$q(\theta) = 2 \left(\theta - \frac{3\pi}{10} - \frac{2\pi}{5}j \right)^2 + \frac{4}{9}, \quad \theta \in \left[\frac{\pi}{10} + \frac{2\pi}{5}j, \frac{\pi}{2} + \frac{2\pi}{5}j \right), \quad j = 0, 1, 2, 3, 4.$$

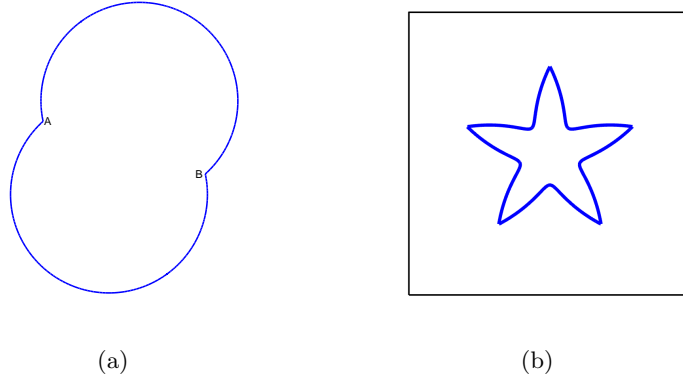


Figure 4.1: The computational domain of Example 1 (left) and Example 2 (right).

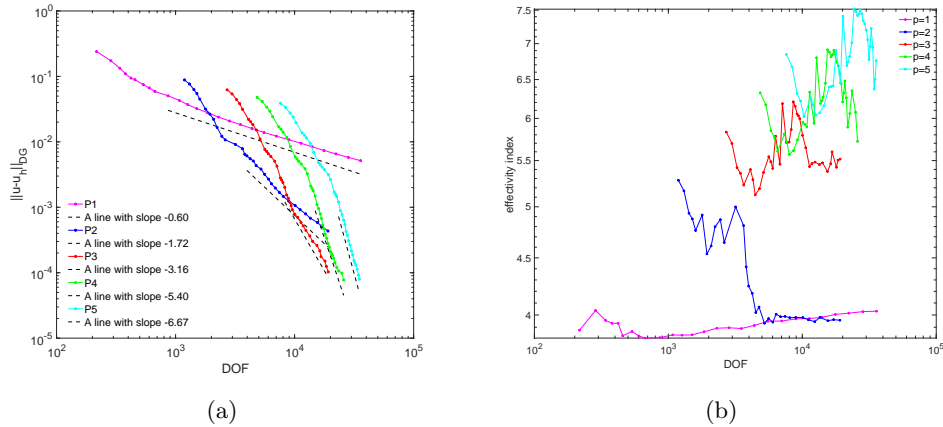


Figure 4.2: Example 1: The exact solution is u_1 . The quasi-optimal decay of the error of the adaptive solutions for $p = 1, 2, 3, 4, 5$ (left) and the effectivity index against #DoFs for $p = 1, 2, 3, 4, 5$ (right).

The coefficient a in (2.1)-(2.2) is taken as $a_1 = 10, a_2 = 1$. We take the source $f_1 = 1, f_2 = \cos(20x_1x_2)$, and boundary condition $g = 0$.

Fig.4.5 shows the quasi-optimal convergence the adaptive solutions when $f_1 = 1$ (left) and $f_2 = \cos(20x_1x_2)$ (right). We again observe the decay is faster than the quasi-optimal decay of the high-order methods $p = 2, 3, 4, 5$, when $f_1 = 1$. On the other hand, we observe the quasi-optimal convergence rate of the adaptive solutions when $f_2 = \cos(20x_1x_2)$ for $p = 1, 2, 3, 4, 5$.

Fig.4.6 shows the adaptive meshes for $p = 2, 3, 4$. We observe that the meshes are mainly refined around the sharp corners where the solution is singular. Table 2 shows the error of the high-order methods is much smaller than the low-order method when the #DoFs are almost the same.

Example 3. In this example, as an application of the adaptive high-order unfitted finite

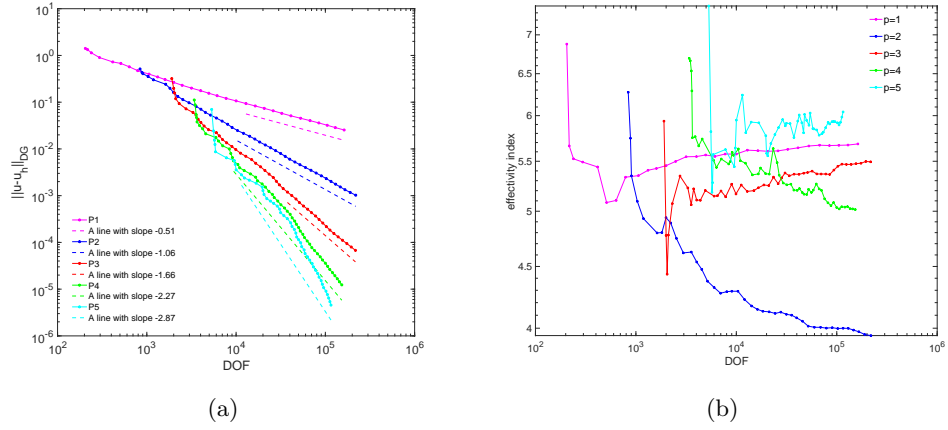


Figure 4.3: Example 1: The exact solution is u_2 . The quasi-optimal decay of the error of the adaptive solutions for $p = 1, 2, 3, 4, 5$ (left) and the effectivity index against #DoFs for $p = 1, 2, 3, 4, 5$ (right).

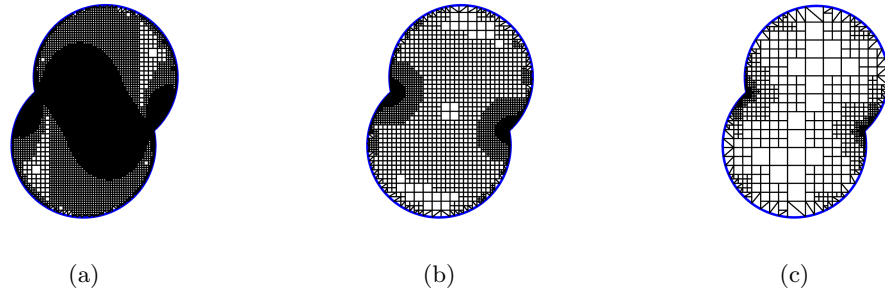


Figure 4.4: Example 1: The adaptive meshes for $p = 1, 2, 3$ when the exact solution is u_1 .

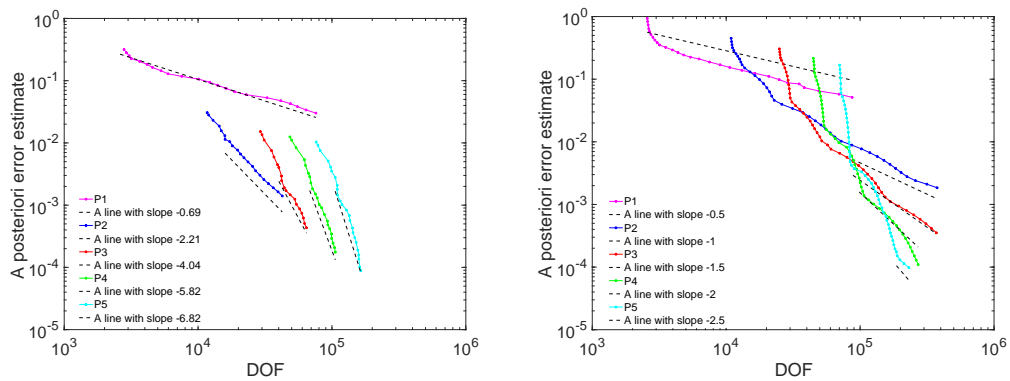


Figure 4.5: Example 2: The quasi-optimal decay of the error of the adaptive solutions for $p = 1, 2, 3, 4, 5$ with $f_1 = 1$ (left) and $f_2 = \cos(20x_1x_2)$ (right).

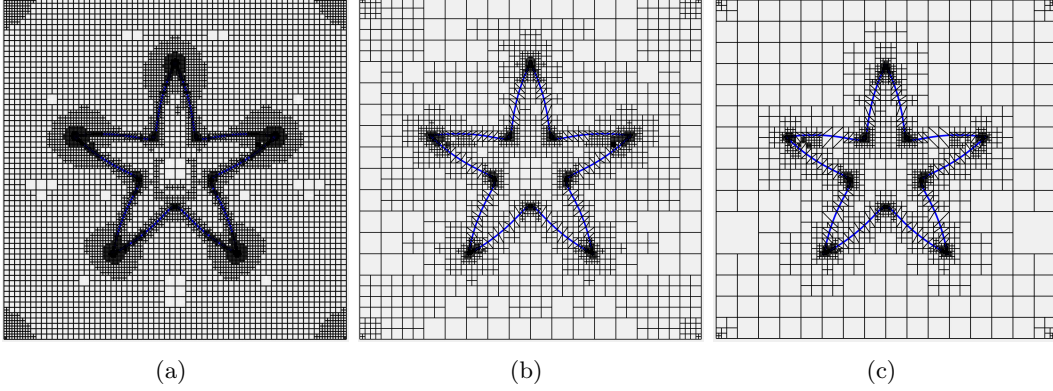


Figure 4.6: Example 2: The adaptive meshes for $p = 2, 3, 4$ when $f_1 = 1$.

	$p = 1$	$p = 3$	$p = 5$
#DoFs	253604	251406	231231
Error	1.87E-02	8.00E-04	9.81E-05

Table 2: Example 2: The error of the numerical solutions and #DoFs when $f_2 = \cos(20x_1x_2)$.

element method developed in this paper, we consider the influence of the geometric modeling error to the solution of elliptic problems. For $i = 1, 2$, let $u_i \in H^1(D_i)$ be the solution of the problem

$$-\Delta u_i = 1 \quad \text{in } D_i, \quad u = 0 \quad \text{on } \partial D_i,$$

where for $b_1 = 1/2, b_2 = \sqrt{3}/2$,

$$D_1 = \{(x_1, x_2) \in (-2, 2)^2 : \alpha|b_1x_1 + b_2x_2| + \beta| -b_2x_1 + b_1x_2| > 1\},$$

$$D_2 = \{(x_1, x_2) \in (-2, 2)^2 : \alpha\sqrt{|b_1x_1 + b_2x_2|^2 + \epsilon} + \beta\sqrt{| -b_2x_1 + b_1x_2|^2 + \epsilon} > 1\}.$$

We have $D_1 \subset D_2$, see Fig.4.7 when $\alpha = \sqrt{5}$, $\beta = \sqrt{2/3}$, and $\epsilon = 0.001$. For $\epsilon > 0$ small, D_1 can be viewed as an approximation of the domain D_2 with round-shaped corners.

The exact solutions of this example are unknown. We use Algorithm 3 to compute the numerical solutions u_h on D_1 and $u_{h,\epsilon}$ on D_2 . The tolerance is set to be $TOL=1.0E-05$ and the finite element approximation order is $p = 5$. Fig.4.8-4.9 depict the computational meshes.

It is easy to see that $|G_1| = |D_2 \setminus \bar{D}_1| = O(\epsilon \log(1/\epsilon))$. The solution u_1 has reentrant corner singularities. It follows from the standard argument (see, e.g., Chen and Wu [23, §4.1]) that $u_1 \in W^{1,p_1}(D_1)$, where $p_1 = 1/(2 - (\pi/\theta))$, $\theta = 2\pi - 2 \arctan(\sqrt{3}/10)$. The solution u_2 is, on the other hand, smooth $u_2 \in W^{1,\infty}(D_2)$. By Theorem 5.1, $\|\nabla(u_1 - u_2)\|_{L^2(D_1)} \leq C(\epsilon \log(1/\epsilon))^\sigma$, $|\nabla(u_1 - u_2)(x_*)| \leq C(\epsilon \log(1/\epsilon))^{2\sigma}$, where $\sigma = (p_1 - 2)/(2p_1) \approx 0.297$, and $x_* = (\sqrt{2}, \sqrt{2})$ that is away from the boundaries of D_1 and D_2 . Fig.4.10 shows

the relative error of the numerical solutions

$$\frac{\|\nabla(u_h - u_{h,\epsilon})\|_{L^2(D_1)}}{\|\nabla u_h\|_{L^2(D_1)}}, \quad \frac{|\nabla(u_h - u_{h,\epsilon})(x_*)|}{|\nabla u_h(x_*)|},$$

which clearly confirms our theoretical findings. We observe that the relative energy error in the whole domain D_1 is about 15% when $\epsilon = 10^{-3}$ but the relative gradient error is rather small away from the corner singularities. This implies that one should be careful if one is interested in the solution u_2 close to the tips of its round-shaped corners. The solution u_1 at these points may not give accurate approximations of u_2 there.

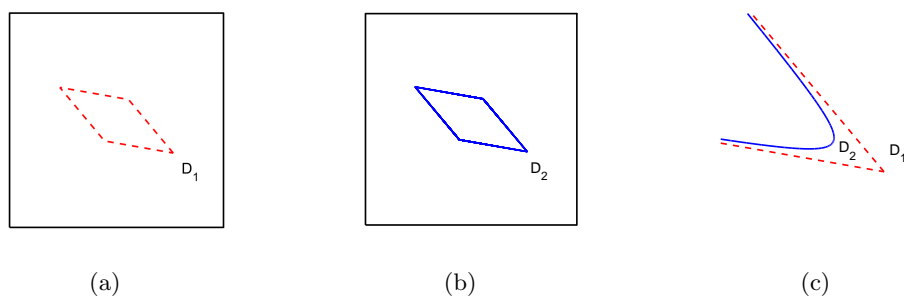


Figure 4.7: Example 3: The computational domain with the sharp corner D_1 (left), with the round shaped corner D_2 (middle), and the local domain near the singular point (right).

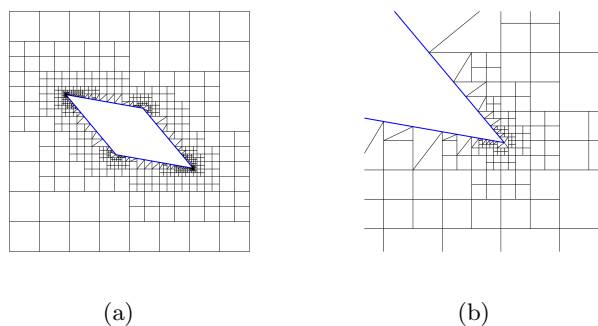
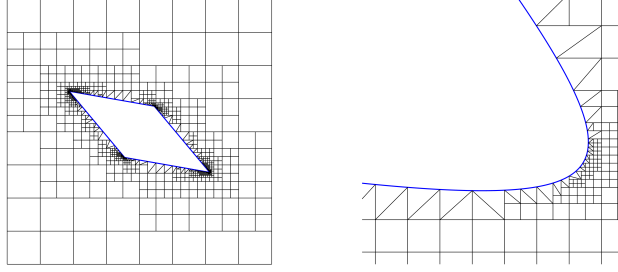


Figure 4.8: Example 3: The computational mesh in D_1 (left) and corresponding local mesh within $(1.056, 1.064) \times (-0.616, -0.608)$ (right).

5 Appendix

In this appendix, we study the influence of the geometric modeling error in the setting of Example 3. Let $D_1, D_2 \subset \mathbb{R}^2$ be two Lipschitz domains so that $D_1 \subset D_2$, see Fig.5.1. Set $G_1 = D_2 \setminus \bar{D}_1$. Let $u_i \in H^1(D_i)$, $i = 1, 2$, be the solution of the problem

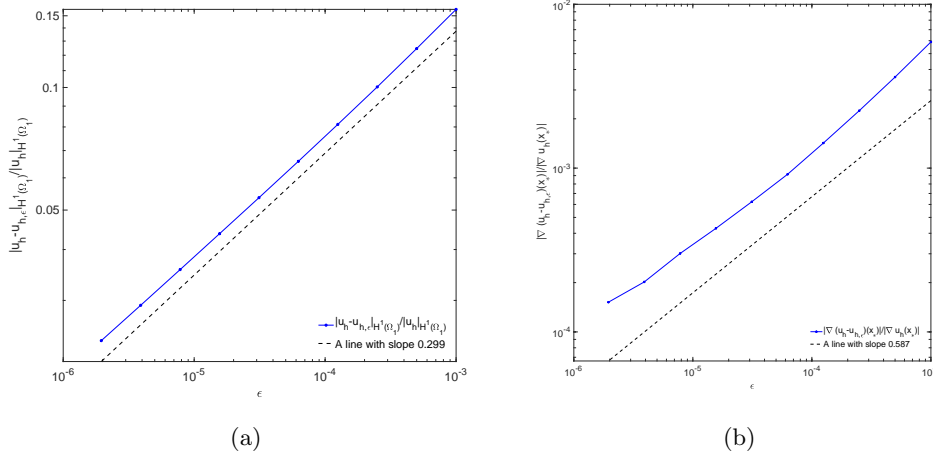
$$-\Delta u_i = f_i \text{ in } D_i, \quad u_i = 0 \text{ on } \partial D_i, \quad (5.1)$$



(a)

(b)

Figure 4.9: Example 3: The computational mesh in D_2 (left) and corresponding local mesh within $(1.054, 1.058) \times (-0.612, -0.608)$ (right).



(a)

(b)

Figure 4.10: Example 3: The relative energy error (left) and the relative error at x_* (right)

where $f_i \in L^2(D_i)$ satisfying $f_2 = f_1$ in D_1 . By Jerison and Kenig [31, Theorem 0.5], there exists $p_i > 2$ such that $u_i \in W^{1,p_i}(D_i)$ and

$$\|u_i\|_{W^{1,p_i}(D_i)} \leq C(p_i, D_i) \|f_i\|_{W^{-1,p_i}(D_i)} \quad (5.2)$$

for some constant $C(p_i, D_i)$ depending on p_i, D_i . Here $W^{-1,p_i}(D_i)$ is the dual space of $W_0^{1,p_i}(D_i)$, where $1/p_i + 1/p_i' = 1$.

Let $B \subset \mathbb{R}^2$ be some circle including D_2 and let $\tilde{f}_2 = f_2 \chi_{D_2}$, where χ_{D_2} is the characteristic function of D_2 . Let $\tilde{u}_1 \in H^1(B \setminus \bar{D}_1)$ be the extension of u_1 with continuing flux such that

$$-\Delta \tilde{u}_1 = \tilde{f}_2 \text{ in } B \setminus \bar{D}_1, \quad \frac{\partial \tilde{u}_1}{\partial n_1} = \frac{\partial u_1}{\partial n_1} \text{ on } \partial D_1, \quad \tilde{u}_1 = 0 \text{ on } \partial B, \quad (5.3)$$

where n_1 is the unit normal to ∂D_1 . Since $u_1 \in W^{1,p_1}(D_1)$, it is easy to see that $\frac{\partial u_1}{\partial n_1} \in W^{-1/p_1, p_1}(\partial D_1)$ and $\|\partial u_1 / \partial n_1\|_{W^{-1/p_1, p_1}(\partial D_1)} \leq C \|u_1\|_{W^{1,p_1}(D_1)}$, where $W^{-1/p_1, p_1}(\partial D_1)$ is

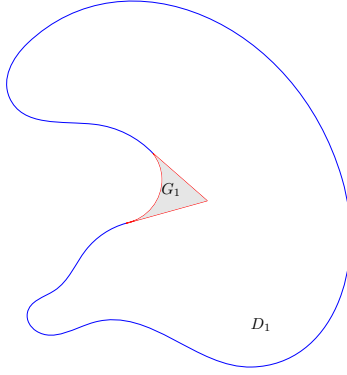


Figure 5.1: Illustration of domains of the problems (5.1).

the dual space of $W^{1/p_1, p_1'}(\partial D_1)$. By Geng [26, Theorem 1.2], if $f_2 \in L^{p_2}(D_2)$, we know that there exists a $q \in (2, \min(p_1, p_2))$, such that

$$\begin{aligned} \|\tilde{u}_1\|_{W^{1,q}(B \setminus \bar{D}_1)} &\leq C(q, D_1) \left(\|\tilde{f}_2\|_{L^q(B \setminus \bar{D}_1)} + \left\| \frac{\partial u_1}{\partial n_1} \right\|_{W^{-1/q, q}(\partial D_1)} \right) \\ &\leq C(q, D_1) (\|f_2\|_{L^q(D_2)} + \|u_1\|_{W^{1,q}(D_1)}), \end{aligned} \quad (5.4)$$

where the constant $C(q, D_1)$ depends on q and $B \setminus \bar{D}_1$. The following theorem is the main result of this appendix.

Theorem 5.1. *Let $\epsilon = |G_1|$ and $\sigma = (q - 2)/(2q)$, where $q \in (2, \min(p_1, p_2))$. If $f_2 \in L^{p_2}(D_2)$ and $u_i, i = 1, 2$, is the solution of (5.1), there exists a constant C independent of $u_i, f_i, i = 1, 2$, such that*

- (i) $\|\nabla(u_1 - u_2)\|_{L^2(D_1)} \leq C\epsilon^\sigma (\|f_1\|_{W^{-1, p_1}(D_1)} + \|f_2\|_{L^{p_2}(D_2)})$;
- (ii) $|\nabla(u_1 - u_2)(x_*)| \leq Cd^{-2}\epsilon^{2\sigma} (\|f_1\|_{W^{-1, p_1}(D_1)} + \|f_2\|_{L^{p_2}(D_2)})$, where $x_* \in D_1$ with $B(x_*, d) \subset D_1$.

Proof. We first show (i). By integrating by parts, since $u_i = 0$ on $\partial D_i, i = 1, 2$, and $\Delta(u_1 - u_2) = 0$ in D_1 , by (5.3) we have

$$\|\nabla(u_1 - u_2)\|_{L^2(D_1)}^2 = - \int_{\partial D_1} \frac{\partial(u_1 - u_2)}{\partial n_1} u_2 = \int_{\partial G_1} \frac{\partial(\tilde{u}_1 - u_2)}{\partial n} u_2, \quad (5.5)$$

where n is the unit outer normal to ∂G_1 . By Hölder inequality, for any $q > 2$, $\|v\|_{L^2(G_1)} \leq \epsilon^\sigma \|v\|_{L^q(G_1)} \quad \forall v \in L^q(G_1)$. Now since $\Delta(\tilde{u}_1 - u_2) = 0$ in G_1 , it follows from (5.5), (5.1) and (5.4) that

$$\begin{aligned} \|\nabla(u_1 - u_2)\|_{L^2(D_1)}^2 &= \int_{G_1} \nabla(\tilde{u}_1 - u_2) \cdot \nabla u_2 \leq \epsilon^{2\sigma} \|\nabla(\tilde{u}_1 - u_2)\|_{L^q(G_1)} \|\nabla u_2\|_{L^q(G_1)} \\ &\leq C\epsilon^{2\sigma} (\|f_1\|_{W^{-1, q}(D_1)} + \|f_2\|_{L^q(D_2)})^2. \end{aligned} \quad (5.6)$$

This shows (i) as $q \leq \min(p_1, p_2)$. To prove (ii), we use the interior gradient estimate for harmonic functions (see e.g., Axler et al. [3, Corollary 8.2]) to obtain $|\nabla(u_1 - u_2)(x_*)| \leq$

$Cd^{-2}\|u_1 - u_2\|_{L^2(D_1)}$. Now we estimate $\|u_1 - u_2\|_{L^2(D_1)}$ by the duality argument. First we note that

$$\int_{D_1} \nabla(u_1 - u_2) \cdot \nabla v = 0 \quad \forall v \in H_0^1(D_1). \quad (5.7)$$

Let $w_j \in H_0^1(D_j)$, $j = 1, 2$, be the solution of the problems

$$-\Delta w_1 = u_1 - u_2 \quad \text{in } D_1, \quad -\Delta w_2 = (u_1 - u_2)\chi_{D_1} \quad \text{in } D_2, \quad (5.8)$$

where χ_{D_1} is the characteristic function of D_1 . By (5.1) we have for $i = 1, 2$,

$$\|w_i\|_{W^{1,q}(D_i)} \leq C\|w_i\|_{W^{1,p_i}(D_i)} \leq C\|u_1 - u_2\|_{W^{-1,p_i}(D_1)} \leq C\|u_1 - u_2\|_{L^2(D_1)}. \quad (5.9)$$

By (5.6) and (5.2) we have

$$\begin{aligned} \|\nabla(w_1 - w_2)\|_{L^2(D_1)} &\leq C\epsilon^\sigma(\|u_1 - u_2\|_{W^{-1,q}(D_1)} + \|u_1 - u_2\|_{L^q(D_1)}) \\ &\leq C\epsilon^\sigma(\|f_1\|_{W^{-1,p_1}(D_1)} + \|f_2\|_{L^{p_2}(D_2)}). \end{aligned} \quad (5.10)$$

Moreover, by (5.1), $\|w_2\|_{W^{1,p_2}(D_2)} \leq C\|u_1 - u_2\|_{L^2(D_1)}$. By the second equation in (5.8)

$$\|u_1 - u_2\|_{L^2(D_1)}^2 = - \int_{D_1} \Delta w_2 (u_1 - u_2) = \int_{D_1} \nabla w_2 \cdot \nabla (u_1 - u_2) - \int_{\partial D_1} \frac{\partial w_2}{\partial n_1} u_2. \quad (5.11)$$

By (5.8), (5.10) and (i) we have

$$\begin{aligned} \int_{D_1} \nabla w_2 \cdot \nabla (u_1 - u_2) &\leq \|\nabla(w_1 - w_2)\|_{L^2(D_1)} \|\nabla(u_1 - u_2)\|_{L^2(D_1)} \\ &\leq C\epsilon^{2\sigma}(\|f_1\|_{W^{-1,p_1}(D_1)} + \|f_2\|_{L^{p_2}(D_2)})^2. \end{aligned} \quad (5.12)$$

Again, since $u_2 = 0$ on ∂D_2 , $\Delta w_2 = 0$ in G_1 , by (5.9) we obtain

$$\begin{aligned} - \int_{\partial D_1} \frac{\partial w_2}{\partial n_1} u_2 &= \int_{\partial G_1} \frac{\partial w_2}{\partial n} u_2 = \int_{G_1} \nabla u_2 \cdot \nabla w_2 \\ &\leq C\epsilon^{2\sigma} \|u_2\|_{W^{1,q}(G_1)} \|w_2\|_{W^{1,q}(G_1)} \\ &\leq C\epsilon^{2\sigma} \|f_2\|_{W^{-1,p_2}(D_2)} \|u_1 - u_2\|_{L^2(D_1)}. \end{aligned} \quad (5.13)$$

Inserting (5.12)-(5.13) into (5.11) we obtain

$$\|u_1 - u_2\|_{L^2(D_1)} \leq C\epsilon^{2\sigma}(\|f_1\|_{W^{-1,p_1}(D_1)} + \|f_2\|_{L^{p_2}(D_2)}).$$

This completes the proof. \square

References

- [1] S. Adjerid, M. Aiffa, and J.E. Flaherty, Hierarchical finite element bases for triangular and tetrahedral elements, *Comput. Meth. Appl. Mech. Engrg.*, 190, 2925–2941, 2001.
- [2] M. Ainsworth and B. Senior, Aspects of an adaptive hp -finite element method: Adaptive strategy, conforming approximation and efficient solvers, *Comput. Meth. Appl. Mech. Engrg.*, 150, 65–87, 1997.

- [3] S. Axler, P. Bourdon, and R. Wade, *Harmonic Function Theory*, Springer Science & Business Media, 2013.
- [4] I. Babuška, A. Craig, J. Mandel, and J. Pitäranta, Efficient preconditioning for the p version finite element method in two dimension, *SIAM J. Numer. Anal.*, 28, 624–661, 1991.
- [5] I. Babuška and A. Miller, A feedback finite element method with a posteriori error estimation, Part I. The finite element method and some basic properties of the a posteriori error estimator, *Comput. Meth. Appl. Mech. Engrg.*, 61, 1–40, 1987.
- [6] I. Babuška and W. C. Rheinboldt, Error estimates for adaptive finite element computations, *SIAM J. Numer. Anal.*, 15, 736–754, 1978.
- [7] S. Badia, E. Neiva, and F. Verdugo, Robust high-order unfitted finite elements by interpolation based discrete extension, *Comput. Math. Appl.*, 127, 105–126, 2022.
- [8] S. Badia, F. Verdugo, A. F. Martín, The aggregated unfitted finite element method for elliptic problems, *Comput. Methods Appl. Mech. Engrg.*, 336, 533–553, 2018.
- [9] E. Bänsch, Local mesh refinement in 2 and 3 dimensions, *Impact Comput. Sci. Eng.*, 3, 181–191, 1991.
- [10] T. Belytschko, N. Moës, S. Usui, and C. Parimi, Arbitrary discontinuities in finite elements, *Internat. J. Numer. Methods Engrg.*, 50, 993–1013, 2001.
- [11] P. Binev, W. Dahmen, and R. DeVore, Adaptive finite element methods with convergence rates, *Numer. Math.*, 97, 219–268, 2004.
- [12] A. Bonito and R.H. Nochetto, Quasi-optimal convergence rate of an adaptive discontinuous Galerkin method, *SIAM J. Numer. Anal.*, 48, 734–771, 2010.
- [13] E. Burman, M. Cicuttin, G. Delay, and A. Ern, An unfitted hybrid high-order method with cell agglomeration for elliptic interface problems, *SIAM J. Sci. Comput.*, 43, A859–A882, 2021.
- [14] E. Burman and A. Ern, An unfitted hybrid high-order method for elliptic interface problems, *SIAM J. Numer. Anal.*, 56, 1119–1140, 2018.
- [15] E. Burman and P. Hansbo, Fictitious domain finite element methods using cut elements, I. A stabilized Lagrange multiplier method, *Comput. Meth. Appl. Mech. Engrg.*, 199, 2680–2686, 2010.
- [16] E. Burman and P. Hansbo, Fictitious domain finite element methods using cut elements, II. A stabilized Nitsche method, *Appl. Numer. Math.*, 62, 328–341, 2012.
- [17] E. Burman, C. He, and M.G. Larson. A posteriori error estimates with boundary correction for a cut finite element method, *IMA J. Numer. Anal.*, 42, 333–362, 2022.
- [18] J.M. Cascon, C. Kreuzer, R.H. Nochetto, and K.G. Siebert, Quasi-optimal convergence rate for an adaptive finite element method, *SIAM J. Numer. Anal.*, 46, 2524–2550, 2008.

- [19] Z. Chen, K. Li, and X. Xiang, An adaptive high-order unfitted finite element method for elliptic interface problems, *Numer. Math.*, 149, 507–548, 2021.
- [20] Z. Chen and Y. Liu, An arbitrarily high order unfitted finite element method for elliptic interface problems with automatic mesh generation, *J. Comput. Phys.*, 491, 112384, 2023.
- [21] Z. Chen, Y. Liu, and X. Xiang, A high order explicit time finite element method for the acoustic wave equation with discontinuous coefficients, arXiv:2112.02867v2.
- [22] Z. Chen, Y. Xiao, and L. Zhang, The adaptive immersed interface finite element method for elliptic and Maxwell interface problems, *J. Comput. Phys.*, 228, 5000–5019, 2019.
- [23] Z. Chen and H. Wu, Selected Topics in Finite Element Methods, Science Press, Beijing, 2010.
- [24] B. Cockburn and C.-W. Shu, The local discontinuous Galerkin finite element method for time-dependent convection-diffusion systems, *SIAM J. Numer. Anal.*, 35, 2440–2463, 1998.
- [25] A. Ern and M. Vohralik, Polynomial-degree-robust a posteriori estimates in a unified setting for conforming, nonconforming, discontinuous Galerkin, and mixed discretizations, *SIAM J. Numer. Anal.*, 53, 1058–1081, 2015.
- [26] J. Geng, $W^{1,p}$ estimates for elliptic problems with Neumann boundary conditions in Lipschitz domains, *Adv. Math.*, 229, 2427–2448, 2012
- [27] C. Gürken, S. Stiecko, and A. Massing, Stabilized cut discontinuous Galerkin method for advection-reaction problems, *SIAM J. Sci. Comput.*, 42, A2620–2654, 2020.
- [28] A. Hansbo and P. Hansbo, An unfitted finite element method, based on Nitsche’s method, for elliptic interface problems, *Comput. Meth. Appl. Mech. Engrg.*, 191, 5537–5552, 2002.
- [29] C. He and X. Zhang, Residual-based a posteriori error estimation for immersed finite element methods, *J. Sci. Comput.*, 81, 2051–2079, 2019.
- [30] P. Huang, H. Wu, and Y. Xiao, An unfitted interface penalty finite element method for elliptic interface problems, *Comput. Meth. Appl. Mech. Engrg.*, 194, 4135–4195, 2005.
- [31] D. Jerison and C.E. Kenig, The inhomogeneous Dirichlet Problem in Lipschitz domains, *J. Func. Anal.*, 130, 161–219, 1995.
- [32] A. Johansson and M. G. Larson, A high order discontinuous Galerkin Nitsche method for elliptic problems with fictitious boundary, *Numer. Math.*, 123, 607–628, 2013.
- [33] O.A. Karakashian and F. Pascal, Convergence of adaptive discontinuous Galerkin approximations of second order elliptic problems, *SIAM J. Numer. Anal.*, 45, 641–665, 2007.

- [34] Z. Li and K. Ito, The immersed interface method: numerical solutions of PDEs involving interfaces and irregular domains, SIAM, Philadelphia, 2006.
- [35] Z. Li, T. Lin, and X. Wu, New Cartesian grid methods for interface problems using finite element formulation, *Numer. Math.*, 96, 61–98, 2003.
- [36] X. Liu, R. P. Fedkiw, and M. Kang, A boundary condition capturing method for Poisson’s equation on irregular domains, *J. Comput. Phys.*, 160, 151–178, 2000.
- [37] J.M. Melenk, hp -interpolation of non-smooth functions and an application to hp -a posteriori error estimation, *SIAM J. Numer. Anal.*, 43, 127–155, 2005.
- [38] J.M. Melenk and B.I. Wohlmuth, On residual-based a posteriori error estimation in hp -FEM, *Adv. Comput. Math.*, 15, 311–331, 2001.
- [39] R. Mittal and G. Iaccarino, Immersed boundary methods, *Annu. Rev. Fluid Mech.*, 37, 239–261, 2005.
- [40] R. Stevenson, The completion of locally refined simplicial partitions created by bisection, *Math. Comp.*, 77, 227–241, 2008.
- [41] B. Szabó and I. Babuška, Introduction to Finite Element Analysis: Formulation, Verification and Validation, John Wiley & Sons, 2011.
- [42] Y. Xiao, J. Xu, and F. Wang, High-order extended finite element method for solving interface problems, *Comput. Meth. Appl. Mech. Engrg.*, 364, 112964, 2020.